

The Journal of **Ancient Egyptian Architecture**

vol. 3, 2018

Numerical modelling and mechanical behaviour analysis of gable vaults in pharaonic construction

Claire Girardeau, Thierry Verdel and
Franck Monnier

Cite this article:

Cl. Girardeau, Th. Verdel and Fr. Monnier, 'Numerical modelling and mechanical behaviour analysis of gable vaults in pharaonic construction', *JAEA* 3, 2018, pp. 65-98.

JAEA

ISSN 2472-999X

Published under Creative Commons CC-BY-NC 2.0

www.egyptian-architecture.com

Numerical modelling and mechanical behaviour analysis of gable vaults in pharaonic construction

Claire Girardeau,¹ Thierry Verdel² and Franck Monnier³

Ancient⁴ Egyptian monumental funerary architecture developed rapidly from the reign of pharaoh Djoser in the 3rd dynasty, around 2,650 B.C., until it reached its zenith during the reigns of Khufu and Khafre in the 4th dynasty. The two largest pyramids were built at Giza at that time.⁵ Funerary chambers of the 3rd dynasty were built underground, whereas during the reign of Khufu's father Snefru, at the start of the 4th dynasty, funerary chambers began to be built in the superstructure of pyramids for the first time. Pyramids at Meidum and Dahshur which belonged to Snefru contain chambers built just above the ground level, with access corridors leading down from raised entrances in the sloped faces of the monuments.⁶ Then came the Khufu's pyramid, with a funerary chamber located more than 40 m above the ground, in the middle of the superstructure.⁷ The challenge of raising larger blocks to higher levels was increased by the need to protect the inner passages and chambers from an increasing mass of overlying masonry, reaching several hundred thousand tons in Khufu's monument.

To protect these burial spaces, the Egyptians initially developed monumental corbelled vaults, and subsequently developed equally imposing rafter vaults (also called gable vaults).⁸ The stone rafter vaults found in the majority of pyramids from the 4th through the 13th dynasties are among the most impressive structures ever produced by the Egyptian architects, in response to one of the most significant technical challenges they encountered.⁹

Traditional arches are made up of several voussoirs held together in compression. Rafter vaults are effectively simple arches, composed of pairs of voussoirs in the form of two sloping beams, facing each other to form a structure shaped like an inverted V.¹⁰ In most cases, distinct rafters are juxtaposed next to each other to form a thick apexed roof, which is described structurally as a type

1 GeoRessources Laboratory, CNRS, University of Lorraine, Mines Nancy, Nancy, France (claire.girardeau@mines-nancy.org).

2 GeoRessources Laboratory, CNRS, University of Lorraine, Mines Nancy, Nancy, France (thierry.verdel@mines-nancy.univ-lorraine.fr).

3 monnierfranck@hotmail.com.

4 Thanks to David Ian Lightbody, JAEA co-editor for technical editing and translation of this article into English.

5 Monnier (2017), pp. 112-147, 166-189.

6 Maragioglio and Rinaldi (1964), pp. 6-53, tav. 2-4 and pp. 124-139, tav. 18-19; Petrie (1892); Dorner (1986), p. 56, fig. 4.

7 Maragioglio and Rinaldi (1965), tav. 2; Dormion (1996), pl. 5.

8 The term commonly used in French is 'Voûte en chevrons' (Monnier (2013), pp. 129-130), which can be translated as 'rafter vault' and also 'gable-roof vault'.

9 Monnier (2014).

10 El-Naggar (1999), pp. 11-12.

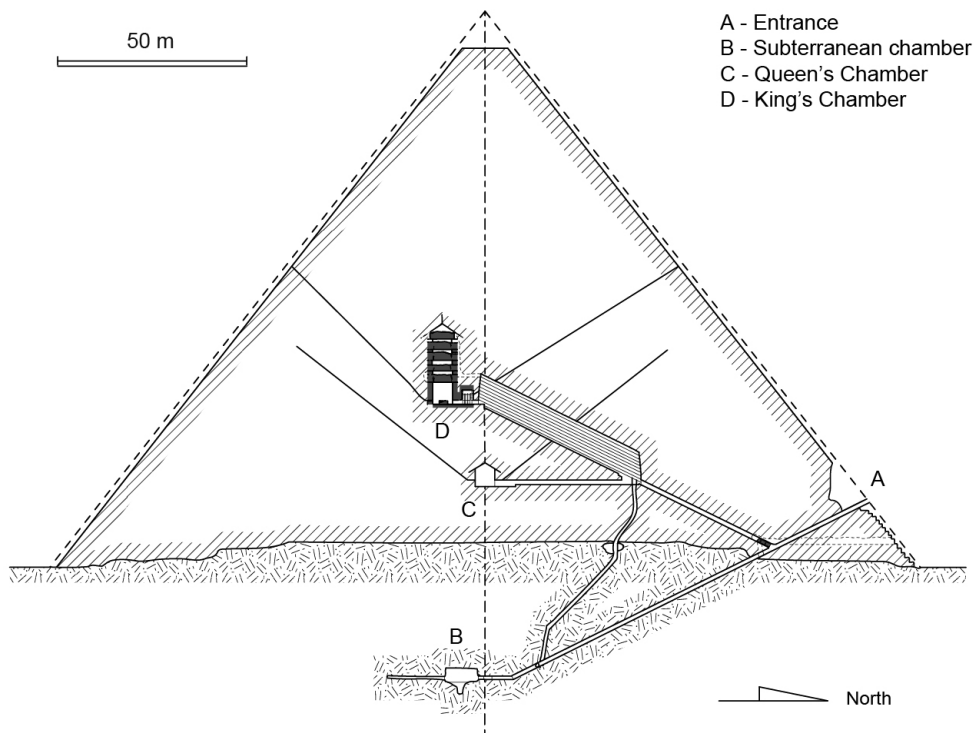


Fig. 1a. Position of the saddle vaults in the Great Pyramid of Khufu: the entrance (A), the Queen's Chamber (C) and the King's Chamber (D).

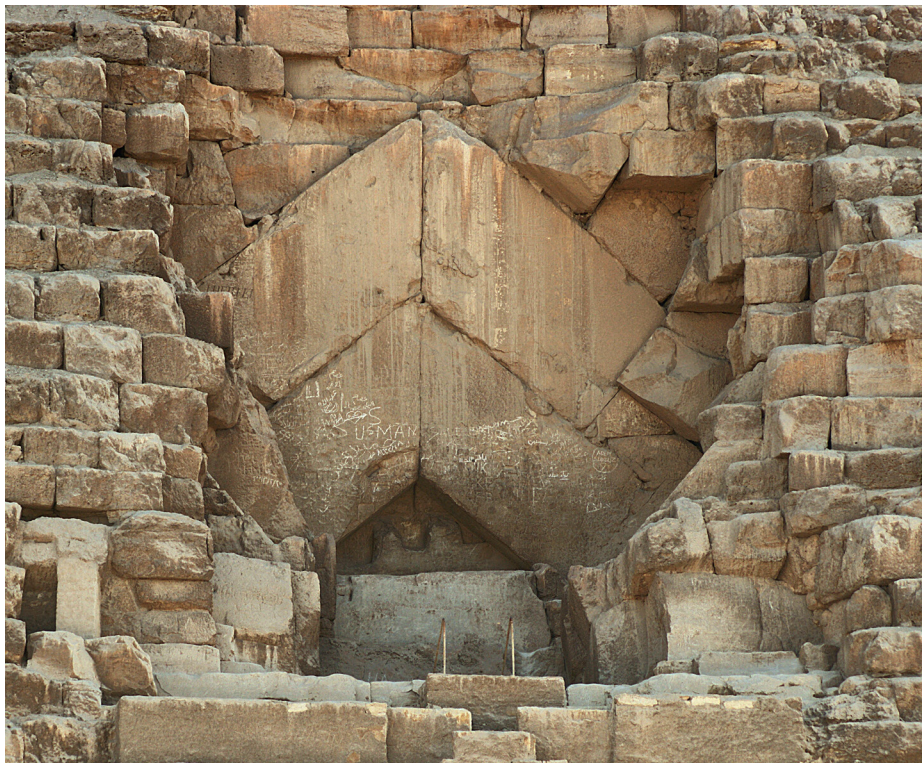


Fig. 1b. Stone rafter vault covering the entrance to the Great Pyramid.
(Franck Monnier)

of vault. Several layers of rafters can also be superimposed. This study addresses single-layer and double-layer vaults, although it should be noted that triple-layer vaults were occasionally used in ancient Egyptian monuments (fig. 1).

Many studies have addressed the mechanical behaviour of masonry vaults and arches,¹¹ but few have dealt with solid stone rafters. The purpose of this article is to investigate their mechanical behaviour using the distinct element method and associated numerical tools. The article is not intended to be a definitive or a comprehensive research report, but a presentation of initial results, and a demonstration of the potential of this approach as an aid to the study of ancient Egyptian architectural structures.

Study background

The theoretical study of the gable vaults drew on methods developed to study classic masonry arches, as rafter vaults function as simple two-vousoir arches. In 1969, Heyman introduced plastic-limit analysis to the study of masonry structures.¹² His methodology assumes that the material and structure have the following properties:

- The structure has no tensile strength, i.e., joints between voussoirs separate on tension. This is a reasonable assumption as joints between voussoirs are typically dry or contain only weak mortar, and the assumption of no tensile strength tends on the 'safe' side, i.e. the vaults are always assumed to be weaker than they may in fact be in reality.
- The stone is assumed to have an infinite compressive strength. This assumption tends to over-estimate the strength of the stone and is therefore inherently 'unsafe', but it is a reasonable working principle in structures where forces in the material were typically too low for crushing to occur.
- Sliding failure along joints cannot occur. This assumption greatly simplifies the mechanical analysis, even if it is not always realistic.

With the development of computerized modelling and more specifically after the introduction of the distinct element method by Peter Cundall in 1971,¹³ it became possible to take the joints between blocks into account as well as to model large displacements between blocks. The mechanical, numerical, analysis of masonry structures such as arches became possible, producing results that were highly representative of the real structures.

Thrust lines

In an arched structure, the line of thrust is a theoretical line that represents the path of the resultant compressive forces acting on and through the structure from different directions. Arches are stable under their own weight, or under external loads, if we find at least one thrust line lying wholly within the structure, and this holds for individual beams in a gable vault. The example illustrated in figure 2 shows such a thrust line in green in an arrangement similar to the situation experienced by the second layer of beams covering the entrance to Khufu's pyramid. Only one side of the vault is shown in each of the two diagrams.

11 Heyman (1969).

12 Heyman (1969).

13 Cundall (1971).

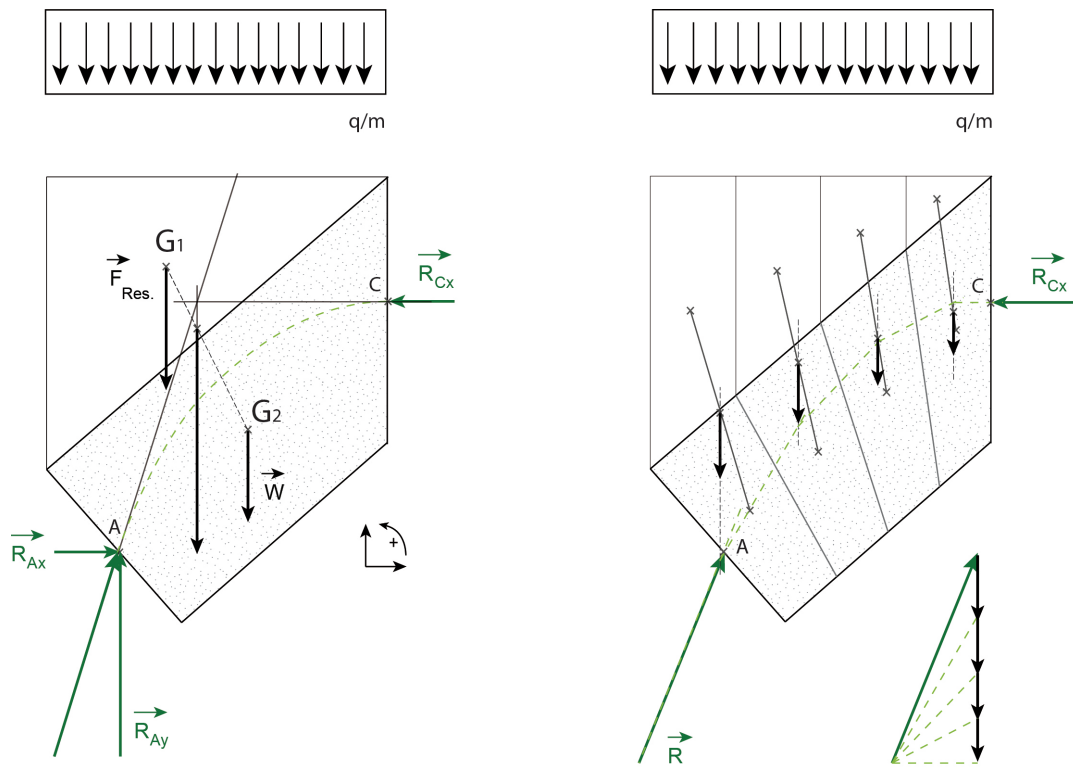


Fig. 2. Loading and possible thrust line in a single rafter such as the upper left one over the entrance to Khufu's pyramid. On the left, the beam is treated as a solid structure, while on the right the beam is evaluated as if it were comprised of 4 separate voussoirs. The forces are resolved for each individual block. The masonry above is simplified and modelled as producing a homogeneous vertical load on the rafter.

In addition to evaluating if the structure is stable, a plastic limit analysis can also determine if the structure will begin to fail, and what the maximum load bearing capacity of the structure might be before that occurred. Using Heyman's simplified assumptions, the maximum load conditions¹⁴ for single span arches are found when one thrust line runs entirely within the masonry but intersects three times with the intrados or the extrados. This extreme limit situation is where the structure satisfies the three conditions for equilibrium but is at the point of collapse. If the arch is not solid then any deflection in this case will lead to the formation of hinge points, and if the structure is loaded up to the point at which it will begin to yield/crush at an interface point, then this state will constitute the maximum global load limit before rupture.

Analysing geometric arrangements and load scenarios by evaluating structures in this extreme situation, however, produces hypothetical situations that are not necessarily representative of reality. Thanks to numerical modelling, more complex geometrical conditions can be studied more easily, and the distinct element method¹⁵ is the most suitable approach for achieving that end. To analyse and better understand the mechanical behaviour of vault rafters the current study follows the methodology established by Idris *et al.*¹⁶ which:

¹⁴ Heyman (1969).

¹⁵ Cundall (1971).

¹⁶ Idris *et al.* (2008).

- Evaluates geometric situations and load cases using distinct element method/UDEC code.
- Defines a safety factor which allows analysis of the mechanical state of the materials.
- Compares different geometries and load cases to understand the overall behaviour of rafters.

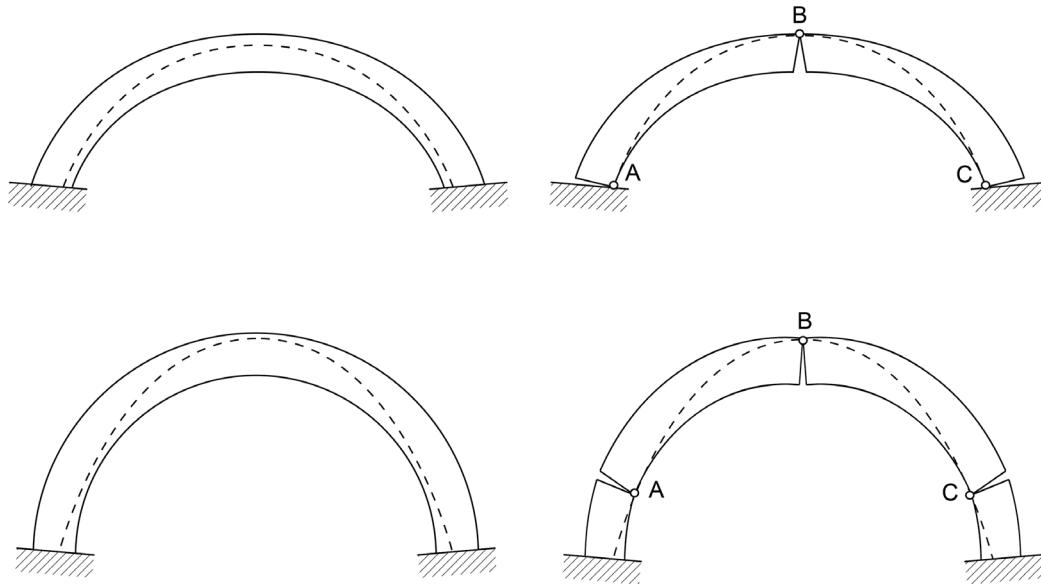


Fig. 3. Thrust line and formation of hinges in a vault.

Numerical modelling methodology

Geometry

During modelling of rafters and their surrounding context, the Universal Distinct Element Code (UDEC) software can analyse systems containing many blocks and interface joints. The modelling is simplified by assuming that the masonry around the rafters is a continuous homogenous material with consistent mechanical properties throughout. This hypothesis is questionable, but greatly simplifies calculations when using this approach. The stiffness of the surrounding matrix is assumed to be low compared to the stiffness of individual continuous blocks, to take the existence of multiple small joints in the surrounding masonry into account.

The structural geometry of gable vaults and their abutment walls on either side was chosen from numerous real-world examples that could have been analysed, as the vaults provided an opportunity to carry out systematic investigation of particular design principles. One of our main objectives was to study the effect of the inclination of the rafters on the performance of the vault. Angle θ was set as a variable, while point A (fig. 4) remains fixed in all models. To model the variable depth of the vault under a masonry superstructure, a homogenous load was applied along the upper boundary of the modelled structure and could be varied according to the depth case being tested. Examples incorporating one or two layers of rafters were investigated. In all cases, the thickness of the different layers of rafters was a constant 2 m while their length changed as the angle of the rafters varied, so

that the span of the vault remained a constant 10 m in every case.¹⁷ The underlying principles of the geometry used are shown in figure 4, which illustrates a case for a two-layer rafter arrangement.

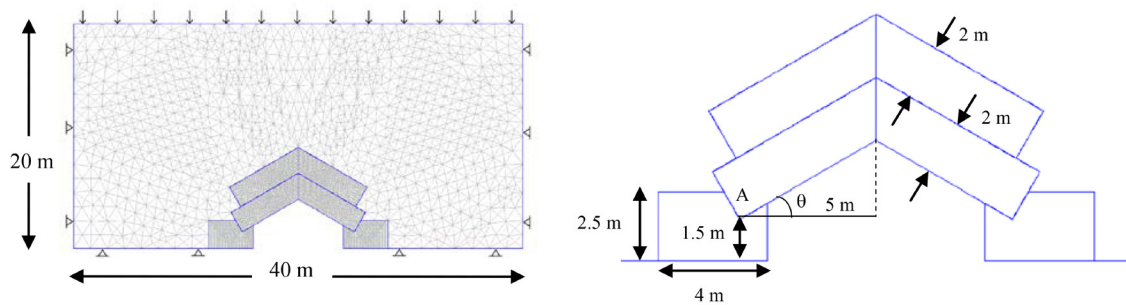


Fig. 4. Model geometry, boundary conditions and mesh.

Mechanical characteristics

To model masonry rafters, the physical and mechanical properties of the stones used for the construction must be realistically represented, while it is assumed that there is no mortar between blocks. This assumption is a safe and realistic hypothesis, as most architectural surveys indicate an absence of mortar in the earlier structures of this kind.¹⁸ Only frictional forces at the interfaces are considered. For the mechanical properties of the stones, pharaonic monuments were mostly constructed using limestone, so available reference values for Young's modulus and Poisson's ratio in limestone were used, as well as reference values relating to friction angles. Information compiled by Nakhla *et al.* regarding the density and compressive strength of limestones from Giza was also used.¹⁹ Since the different reference values varied to some degree, this study used the lowest, which allowed the failure of stones to be more easily observable. Mahrous *et al.* also produced a dataset relating compressive strength to tensile strength for Egyptian limestones, which let us determine an appropriate tensile strength for our modelling.²⁰ Table 1 presents the values selected for the analyses.

Masonry of central structure			Surrounding masonry			Masonry joints		
Parameter	Unit	Value	Parameter	Unit	Value	Parameter	Unit	Value
ρ (Density)	kg/m ³	2050	ρ	kg/m ³	2050	Jkn (normal stiffness)	GPa/m	12
E (Young's modulus)	GPa	12	E	GPa	1.2	Jks (shear stiffness)	GPa/m	4.7
ν (Poisson's ratio)		0.27	ν		0.27	Jc (cohesion)	MPa	0
C (cohesion)	MPa	2	C	MPa	2	$J\phi$ (angle of friction)	°	35
ϕ (angle of friction)	°	35	ϕ	°	35	JTs (tensile strength)	MPa	0
Ts (tensile strength)	MPa	1	Ts	MPa	1			

Table 1. Properties of materials and interface joints used in the modelling (Nakhla *et al.* (2006); Mahrous *et al.* (2010)).

¹⁷ This is a reasonable value to use for the total span width. Even in chambers that are less than 10 m wide, the gable vault extends over and beyond the side walls, which are typically not load bearing.

¹⁸ El-Naggar (1999), pp. 87-129.

¹⁹ Nakhla *et al.* (2006).

²⁰ Mahrous *et al.* (2010).

Numerical modelling results

Introduction of a safety factor

To evaluate the stress levels and identify zones where failure may occur, a safety factor f was calculated. This factor evaluates the stress state in a zone and estimates how close it is to the failure criterion. The calculation of this safety factor follows an established methodology referred to as the Mohr Coulomb failure criterion method. The definition of the factor is represented in figure 5, which follows a graphical convention typical for this type of analysis. In practice, when the factor f falls under 1, there is failure, while a value around 4 shows that there is little or no threat of failure. Coloured bars are displayed under each test case diagram to show the colour coding used to display the safety factor. Red signifies an increased risk of failure as f approaches 1, and yellow indicates a lower risk of failure as f approaches or exceeds 4.

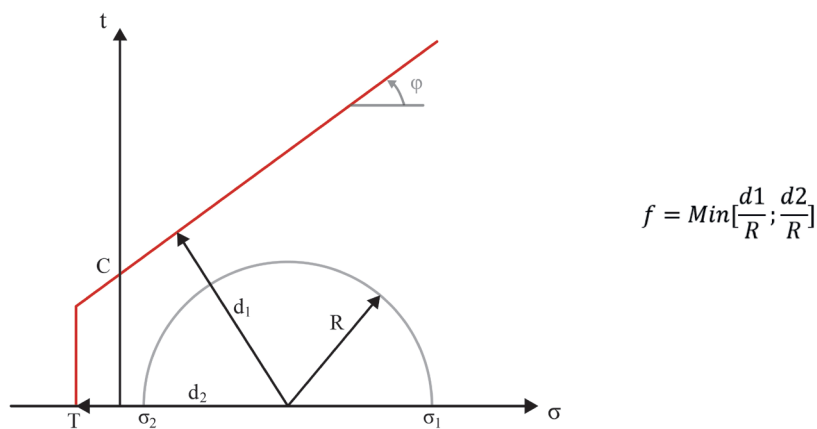


Fig. 5. Safety factor definition, where C is the cohesion, φ the friction angle, and T the tensile strength of the material. σ_1 and σ_2 are the computed maximum and minimum principal stresses.

The calculations were carried out for an isotropic (the material has no characteristic orientation) material with linear elasticity, in a single two-dimensional plane. The section studied was then replicated/extruded over a distance perpendicular to the section, to produce a 3-dimensional model.

The results, including the grid point positions, principal stress values in elements, and stress values at contact points between blocks, were then exported to Mathematica^(R) to be analysed. Only the results for the left rafter(s) and abutment support wall were calculated, as the structures are all symmetrical around the central vertical plane of the model, as would be the stress distribution.

Stress analysis

When loaded, the rafters and abutments walls are subject to distinctive stress distributions with zones that vary significantly between higher and lower stresses. More precisely, it appears that tensile stresses tend to develop along the underside of the rafter, the intrados, towards the upper end where opposing rafters meet. The intensity of the stress in that area increases as the depth of superstructure above increases, or the angle of inclination of the rafter decreases.

This area seems to be the first failure zone encountered when there is a single layer of rafters. When there are two layers of rafters, the first failure zone is located on the intrados of the uppermost

rafter, while the lower rafter exhibits shearing failure zones around the interface with the abutment wall, as well as less severe tensile stress zones on the intrados.

Moreover, the vertical contact surface between pairs of rafters shows relatively high tensile stresses, but these tend to be less severe for the upper layer. Around the abutments, failure tends to occur near the lower contact point with the rafter, which is a highly compressed region. Figure 6 illustrates this behaviour with reference to the safety factor.

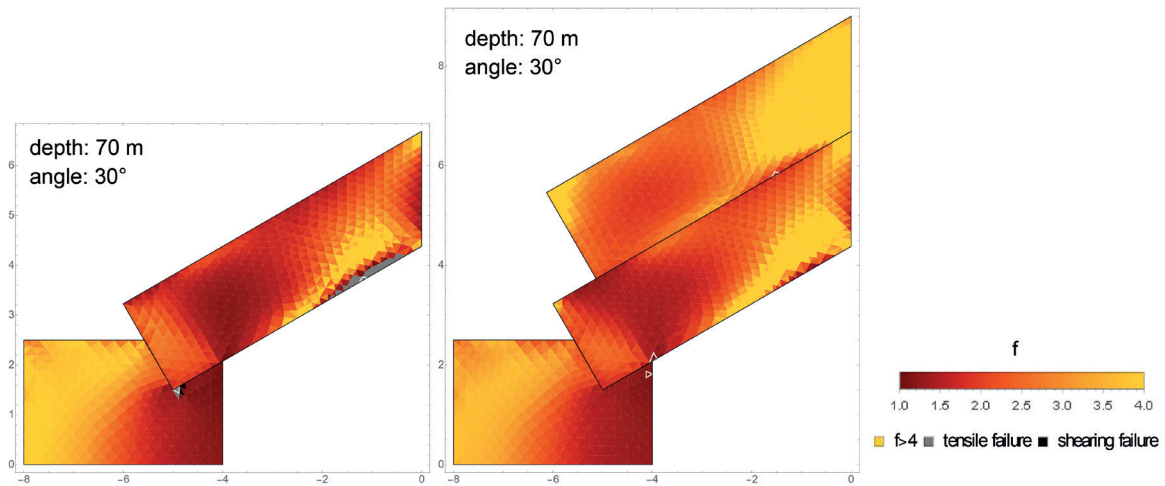


Fig. 6. Safety factor distribution for an angle of 30° and a depth of 70 m (zones highlighted in white have the lowest safety factor experienced by the abutment, or in each rafter).

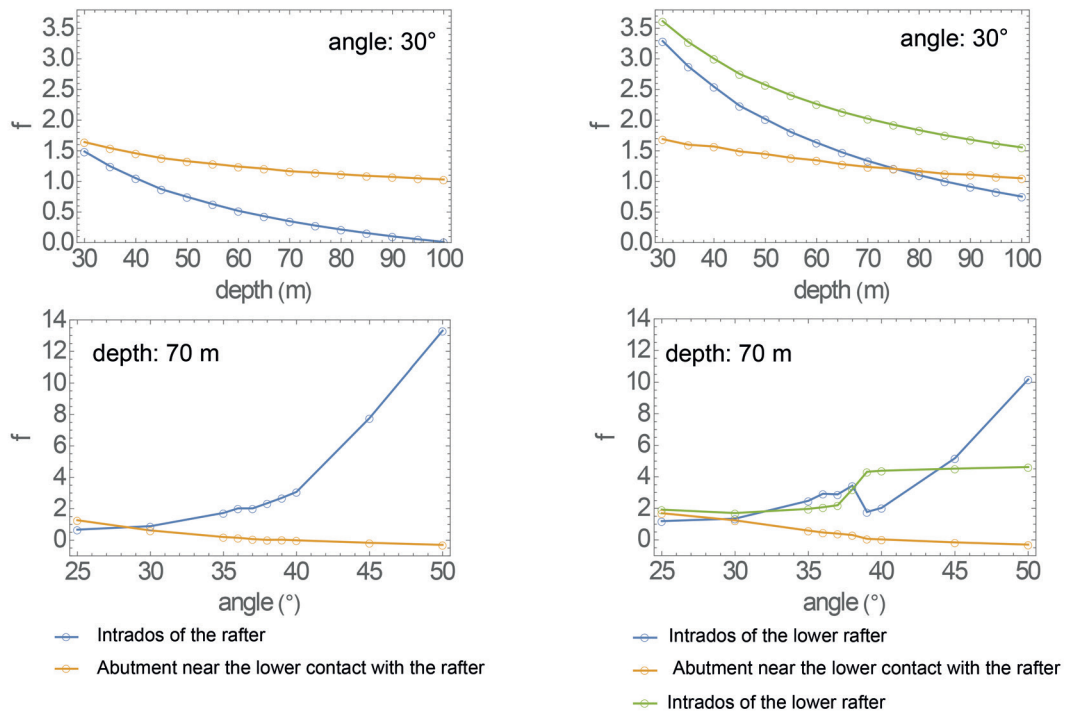


Fig. 7. Depth and angle influence on safety factors for a single-layer rafter vault (left) and double-layer rafter vault (right).

To analyse the effects of the angle of rafters and the depth of the vault under the superstructure, two points in the geometry were chosen that present significant behaviour: a point on the intrados of the rafter that tends to fail in tension (coordinates $\{-1.05, 3.8\}$ or $\{-1.05, 6.1\}$ for 30°) and a point at the lower interface in the abutment (coordinates $\{-4.92, 1.5\}$ for 30°). The safety factor f for these points can then be plotted on a graph, showing how f varies with respect to angle and loading.

Figure 7 shows the influence of the depth and the angle of the vault on the safety factor at these locations. The first behaviour of note is that the deeper the vault is, the lower the safety factors are, regardless of the number of layers or the angles of inclination. The depth, therefore, always increases the failure potential. For a vault with a single layer of rafters, the safety factor of the intrados falls under 1 at a depth of 45 m, whereas with two layers the vault must be 90 m deep before the intrados of the lower rafter will fail. The intrados region, therefore, seems to be less likely to fail when there are multiple layers of rafters. Moreover, the point in the abutment wall displays approximately the same behaviour with one or two layers. The number of rafters does not have a great impact on the behaviour of the abutment interfaces.

The analysis of the influence of the angle of the vault reaches similar conclusions. With one or two layers, the safety factor at the study point in the abutment decreases slowly along with the angle. The angle has the opposite effect on the intrados of the rafters, as the safety factor tends to increase as the angle of the vault increases.

Overall, this means that the intrados may be the initial zone of failure for lower angle vaults, but not for higher angle vaults. For example, for a 70-meter-deep single-layer vault, this region fails first for angles below 35° .

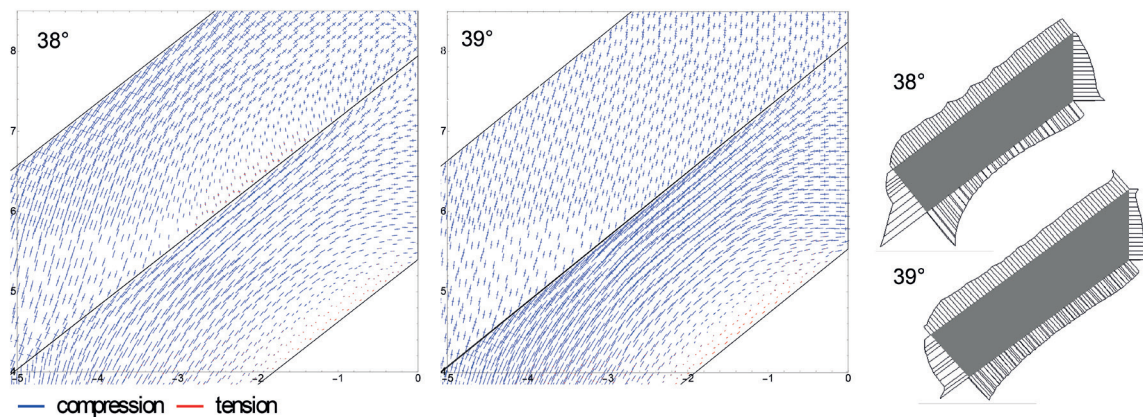


Fig. 8. Principal stress distributions in double-layers rafter vaults at 38° and 39° of inclination, at a depth of 70 m under a superstructure (left); Associated force profiles around the upper rafter, acting normal to the surfaces (right).

With the double-layer vault, a rather sudden drop in the safety factor is visible between 38° and 39° , for the intrados of the lower rafter, while the safety factor of the upper rafter increases around the same angle. This suggests a change in the mechanical behaviour of the rafters that requires some explanation. The illustration of the principal internal stresses experienced by the rafters in figure 8 also shows significant behavior changes in this angle range. For an angle of 38° , the main stresses in the upper rafter exhibit an arch shape showing that some force is being transferred laterally,

while tensile stresses appear close to the intrados. At 39° , the arch form is less obvious in the upper rafter, and most of the principal lateral stresses are carried in the lower rafter. No tensile stresses appear in the upper rafter. The lower rafter is more loaded at 39° , so this transition range seems to indicate a threshold: for angles smaller than this threshold, the upper rafter is compressed and effectively carries loads, but for greater angles it is less compressed and behaves more like a dead weight. The increase in stresses inside the lower rafter around 39° explain the drop of the safety factor on its intrados approaching this angle.

Vertical contact between rafters

The vertical interface joints between rafters on the same layers also displayed interesting behaviour. To analyse this, different parameters were modelled across a range of angles from 25 to 50 degrees. Any opening of the vertical joints, and the normal stress profiles and values of the maximum stresses acting across the interfaces, were plotted. Figure 9 shows how these factors varied according to the angle of the vault, for a vault depth of 45 m.

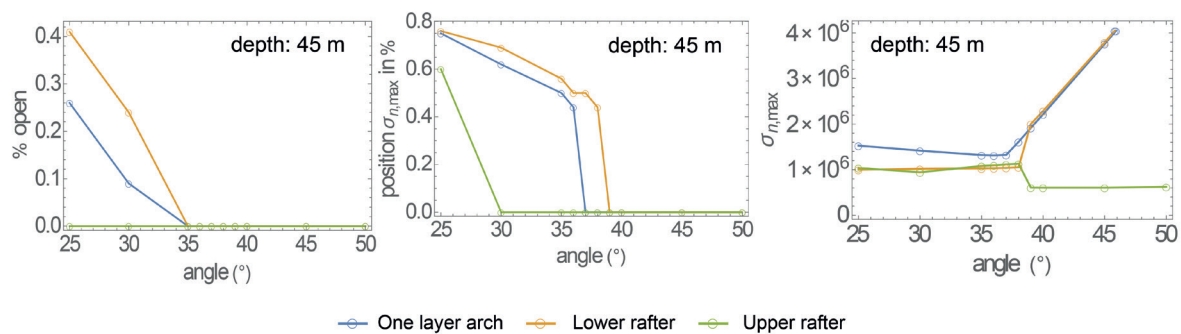


Fig. 9. Angle of rafters related to the opening of gaps (left); maximum normal stress values (right) and position (middle) along the vertical joint between the rafters.

As can be seen with the limestone rafters forming the gable vault above the King's Chamber in the pyramid of Khufu (fig. 10), gaps tend to open at the bottom of the rafter interface joints, as if the beams had dropped downwards slightly on either side. The computational analysis confirms this behaviour, and any openings always appear at the lower extremities of the contact joints modelled. The calculations also show that for rock with the properties modelled, openings only appear at angles below 35° . The real rafters mentioned above, however, have angles of inclination of approximately 40° and yet display some opening, which suggests slightly different masonry characteristics.²¹ Overall, the vaults tend to be more rigid and interface joints remain closed when vault angles increase above these values.

The closure of joints at higher angles can be explained by the displacement of maximum normal stresses toward the bottom of the joints when the angle increases. Moreover, an increased angle also induces a higher value for this maximum on the lower rafter layer. On the upper layer, on the contrary, the value of the maximum normal stress drops between 38° and 39° and this is associated with the overall change in behaviour starting around this value. There is a transfer of loading from the upper rafter to the lower rafter across this angle range.

21 Breitner, Houdin and Brier (2012).

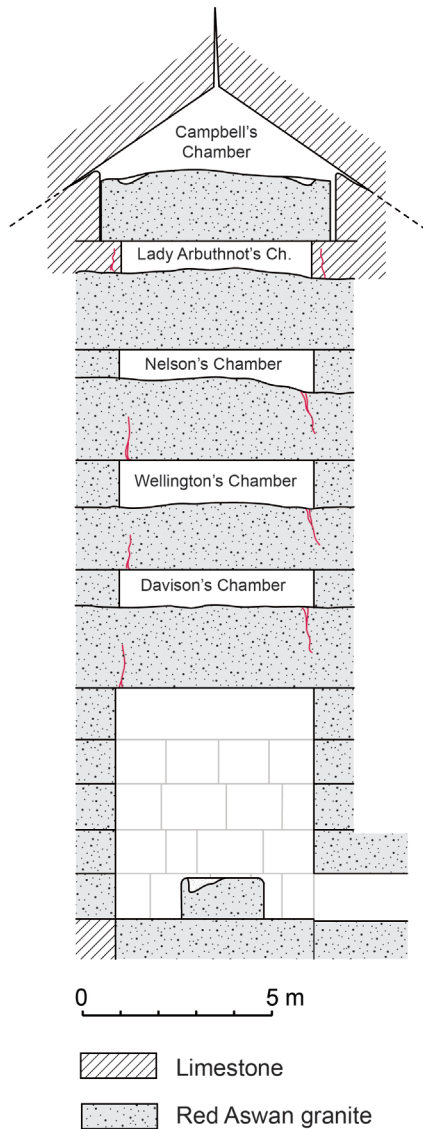


Fig. 10. Illustration of the rafter vault above the King's Chamber in the pyramid of Khufu (after Monnier (2017), fig. 11.44).

Examples of normal stress distributions are given in the Annexes.

The change of these stress and gap parameters with respect to changes in the depth of the superstructure is not particularly notable, as it does not change the stress distribution profile along the joint. The actual values do change, but in direct proportion to the depth. Factors relating depth load and normal stresses increase more rapidly, however, at increased angles. In other words, the higher the angle, the faster the maximum normal stresses increase (see Annexes).

Influence of Young's modulus of the surroundings

In order to analyse the impact of changing Young's modulus in the surrounding matrix, different test cases were repeated with different values of E but without changing the rafter and abutment parameters. The calculations showed that when Young's modulus decreases in the surroundings, then more failure zones appear in the vaults and the openings in the vertical contact joints between the opposing rafters tend to enlarge. As already observed, the arch remains safer if it has two layers. Double-layer vaults also show fewer zones approaching failure and have tighter vertical joints.

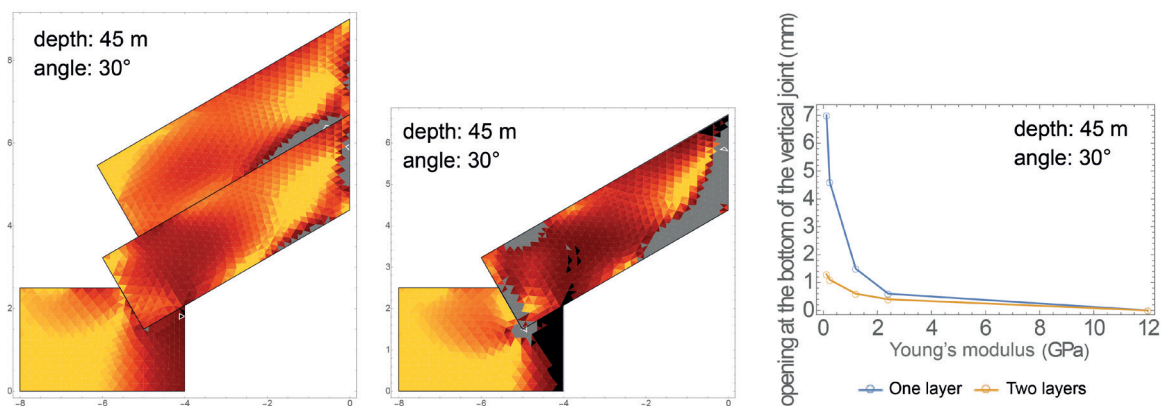


Fig. 11. Safety factor distribution for a Young's modulus of the surroundings of 0.12 GPa and its influence on the opening of the vertical joint.

Conclusion

In this study, we used the distinct element method to model rafter vaults using UDEC software code, then analysed the results with Mathematica^(R). We studied different situations by modifying the number of layers, the inclination of the rafters, the depth of the vault, and Young's modulus in the surrounding matrix. These test cases demonstrated that failures occur in specific areas of the structure such as along the intrados of the rafters, as well as along the vertical joints between opposing rafters, and around the contact zone between the rafters and the abutment walls. The vaults are safer with two layers than with a single layer, although 39° seems to be a threshold value that sees a change in the behaviour of the double-layer vaults. Below this angle the upper rafter effectively carries loads, but above this angle the upper rafter behaves like a dead weight.²² Finally, the vertical openings between rafters increases if the vaults are less inclined, or if Young's modulus in the surrounding matrix is decreased.

These preliminary results will be integrated with additional archaeological data in a forthcoming paper,²³ and it is to be hoped that further research of this kind will be able to more-closely model the behavior of the surrounding masonry and abutments walls.

Bibliography

- Breitner, R., Houdin, J.-P. and Brier, B. (2012), 'A Computer Simulation to Determine When the Beams in the King's Chamber of the Great Pyramid Cracked', *JARCE* 48, pp. 23-33.
- Cundall, P. (1971), *A computer model for simulating progressive, large-scale movements in blocky rock systems*, Proceedings of the International Symposium on Rock Mechanics, Nancy, pp. 129–136.
- Dormion, G. (1996), *Pyramide de Chéops: Architecture des appartements funéraires*, Lyon.
- Dorner, J. (1986), 'Form und Ausmasse der Knickpyramide, Neue Beobachtungen und Messungen', *MDAIK* 42, pp. 43-58.
- El-Naggar, S. (1999), *Les voûtes dans l'architecture de l'Égypte Ancienne*, BdE 128, Cairo, IFAO.
- Gilbert, M. (2007), 'Limit analysis applied to masonry arch bridges: state-of-the-art and recent developments',

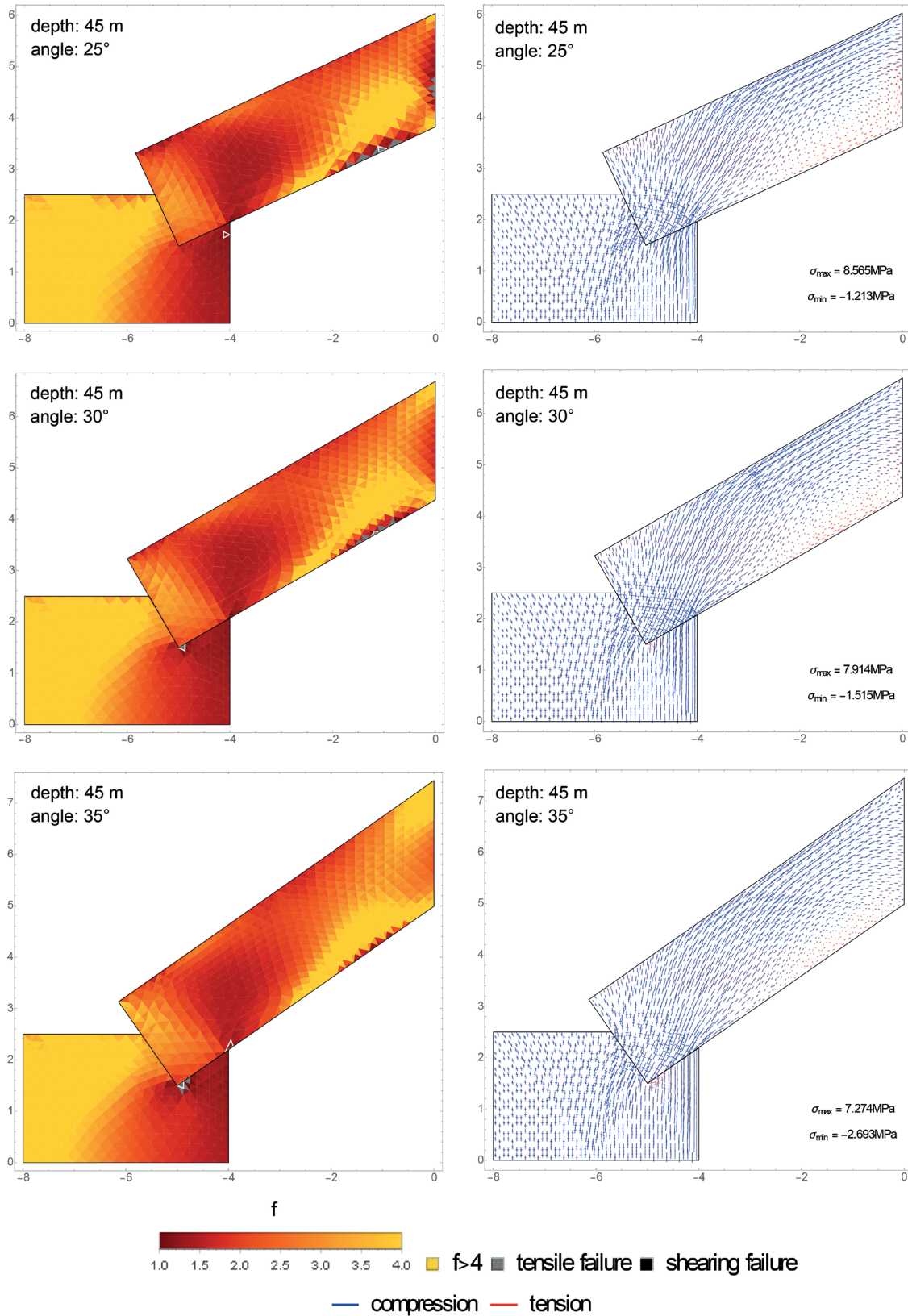
²² Fr. Monnier, 'La voûte en chevrons monumentale. Comportement mécanique, pathologie et évolution', (in press). We can already state that this threshold appears to be a limit value which the ancient Egyptians did not exceed in the earlier pyramids. It is therefore tempting to think that they could have been aware of this behavioral threshold through experience using these types of vaults.

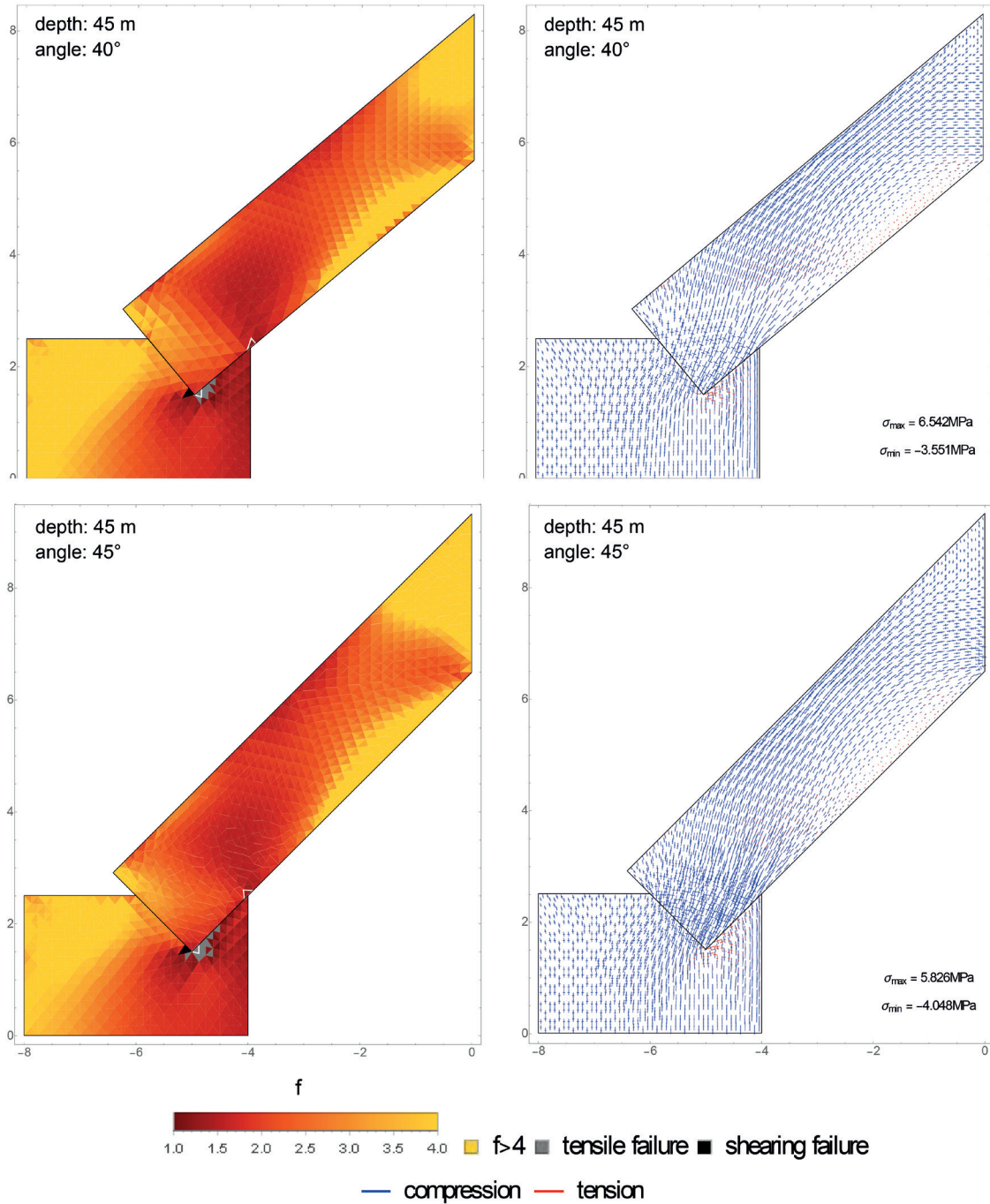
²³ *Ibidem*.

- in P. B. Lourenço, D. B. Oliveira and A. Portela (eds), *Proceedings of the 5th International Conference on Arch Bridges*, Funchal, Madeira: Lda publishers, pp. 13–28.
- Heyman, J. (1969), ‘The Safety of Masonry Arches’, *International Journal of Mechanical Sciences* 11, n° 4, pp. 363–385.
- Idris, J., Verdel, T. and Al-Heib, M. (2008), ‘Numerical modelling and mechanical behaviour analysis of ancient tunnel masonry structures’, *Tunnelling and Underground Space Technology* 23, n° 3, pp. 251–263.
- Mahrous, A. M., Tantawi, M. M. and El-Sageer, H. (2010), ‘Evaluation of the Engineering Properties of Some Egyptian Limestones as Construction Materials for Highway Pavements’, *Construction and Building Materials* 24, n° 12, pp. 2598–2603.
- Nakhla, S. and Abd Elkader, M. (2006), ‘Mortars and Stones for the restoration of masonry works in the sphinx’, In Kh. Daoud and S. Abd el-Fatah (eds), *The world of Ancient Egypt. Essays in honor of Ahmed Abd El-Qader El-Sawi*, Cairo, pp. 207-215.
- Monnier, Fr. (2013), *Vocabulaire d’architecture égyptienne*, Bruxelles.
- Monnier, Fr. (2014), ‘La construction des grandes voûtes en chevrons de l’Ancien Empire’, *GM* 242, pp. 89-104.
- Monnier, Fr. (2017), *L’ère des géants. Une description détaillée des grandes pyramides d’Égypte*, Collection de l’archéologie à l’histoire 67, Paris: De Boccard.
- Maragioglio, V. and Rinaldi, C. (1964), *L’Architettura delle piramidi Menfite. Parte III, Il Complesso di Meydum, la piramide a Doppia Pendenza e la piramide Settentrionale in Pietra di Dabsciur*, Rapallo.
- Maragioglio, V. and Rinaldi, C. (1965), *L’Architettura delle piramidi Menfite. Parte IV, La Grande piramide di Cheope*, Rapallo.
- Maragioglio, V. and Rinaldi, C. (1966), *L’Architettura delle piramidi menfite. Parte V, Le Piramidi di Zedefrà e di Chefren*, Rapallo.
- Maragioglio, V. and Rinaldi, C. (1977), *L’Architettura delle piramidi Menfite. Parte VIII, Le piramidi di Neuserrá, ‘Small Pyramid’, Menkaubor, Isesi*, Turin/Rapallo.
- Petrie Fl., *Medum*, London, 1892.

Annex 1

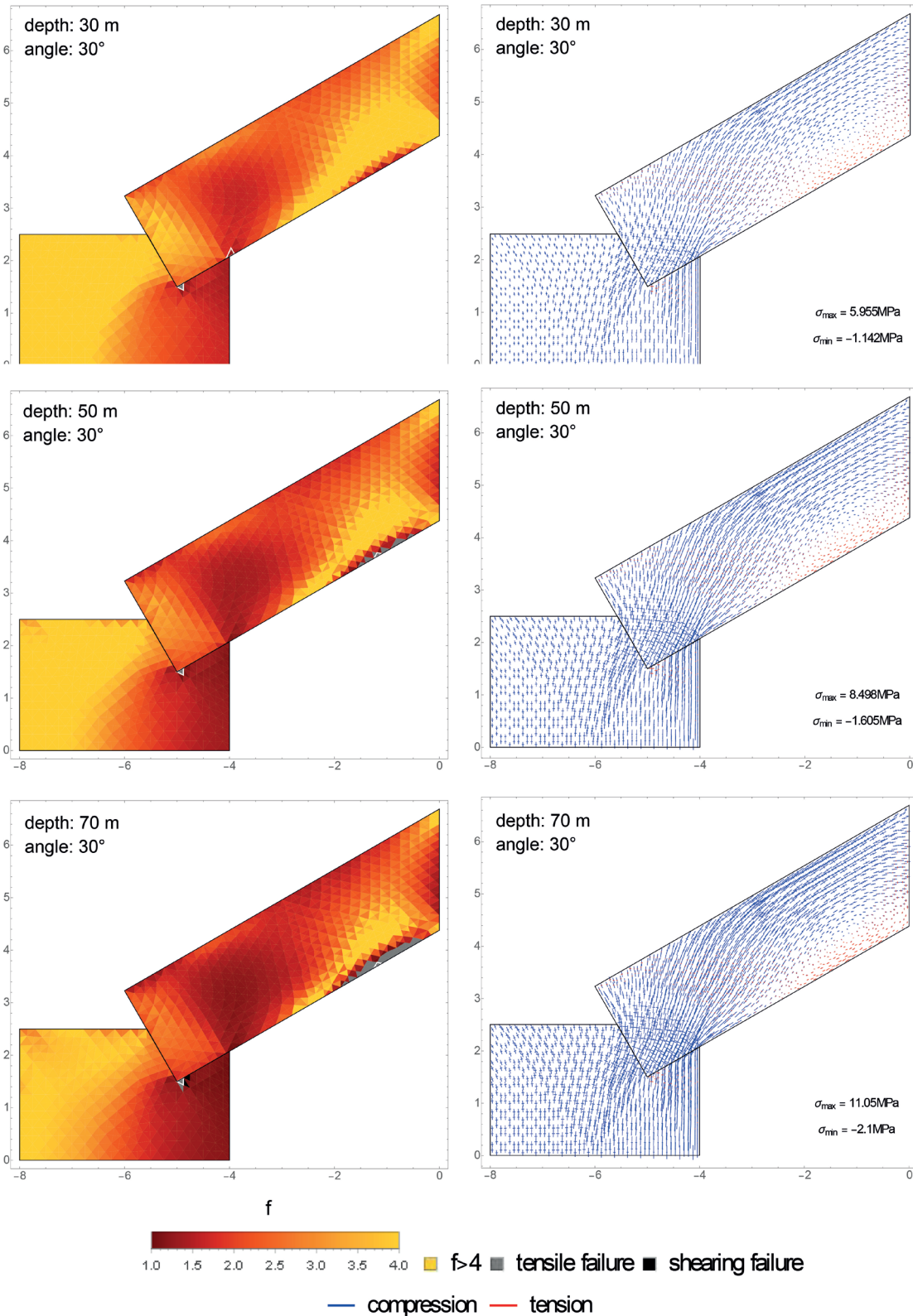
Safety factor and corresponding stress distribution for a single layer of rafters for different angles and a depth of 45 m (zones contoured in white presents the minimum safety factor in the abutment or in the rafter).

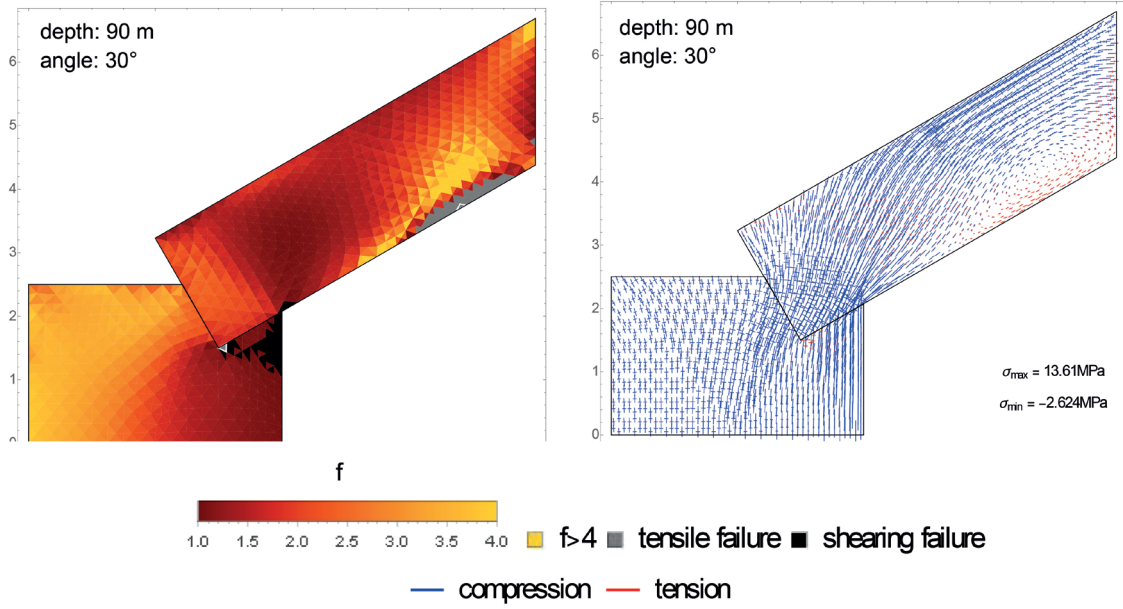




Annex 2

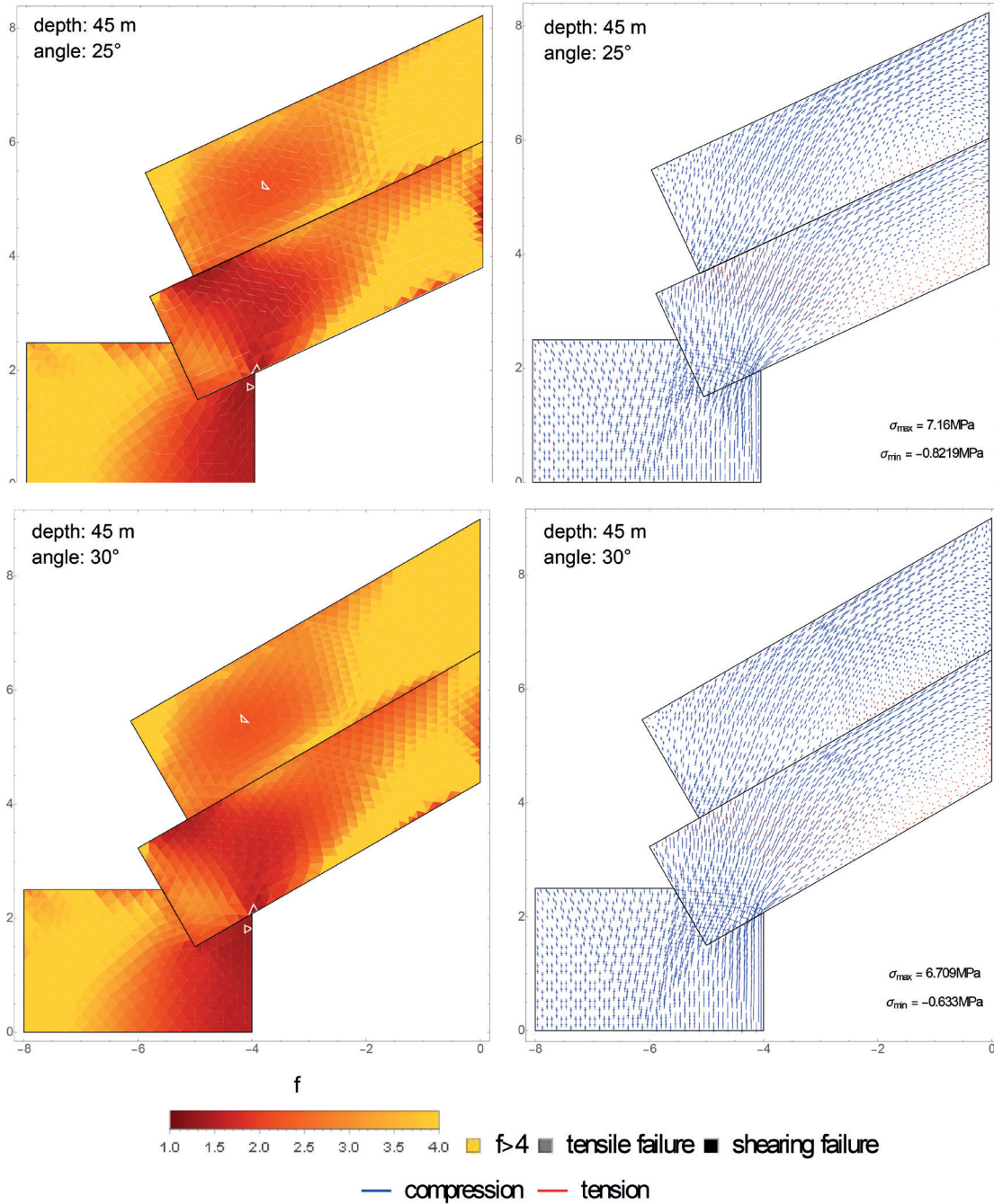
Safety factor and corresponding stress distribution for a single layer of rafters for different depths and an angle of 30° (zones contoured in white presents the minimum safety factor in the abutment or in the rafter).

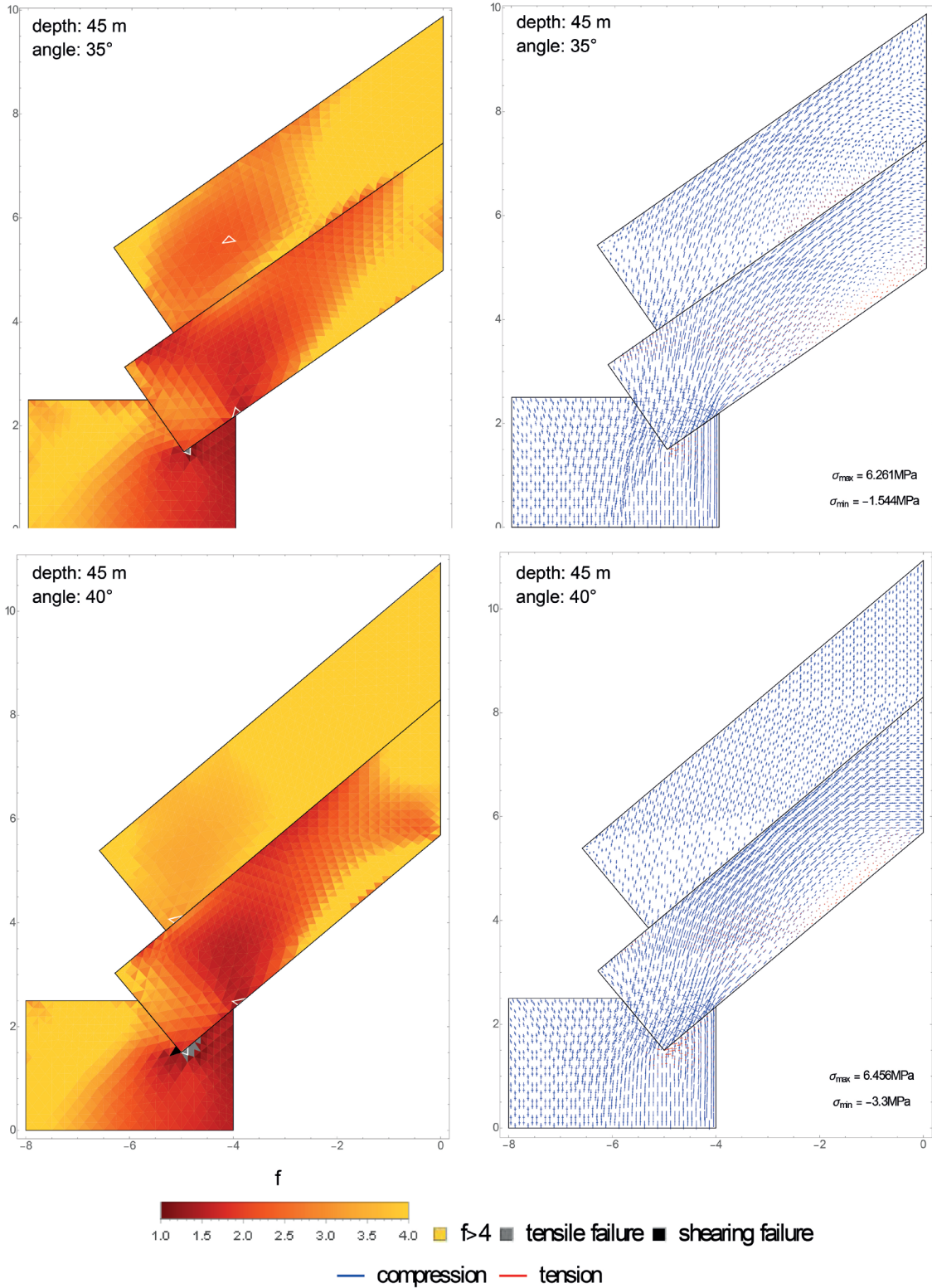


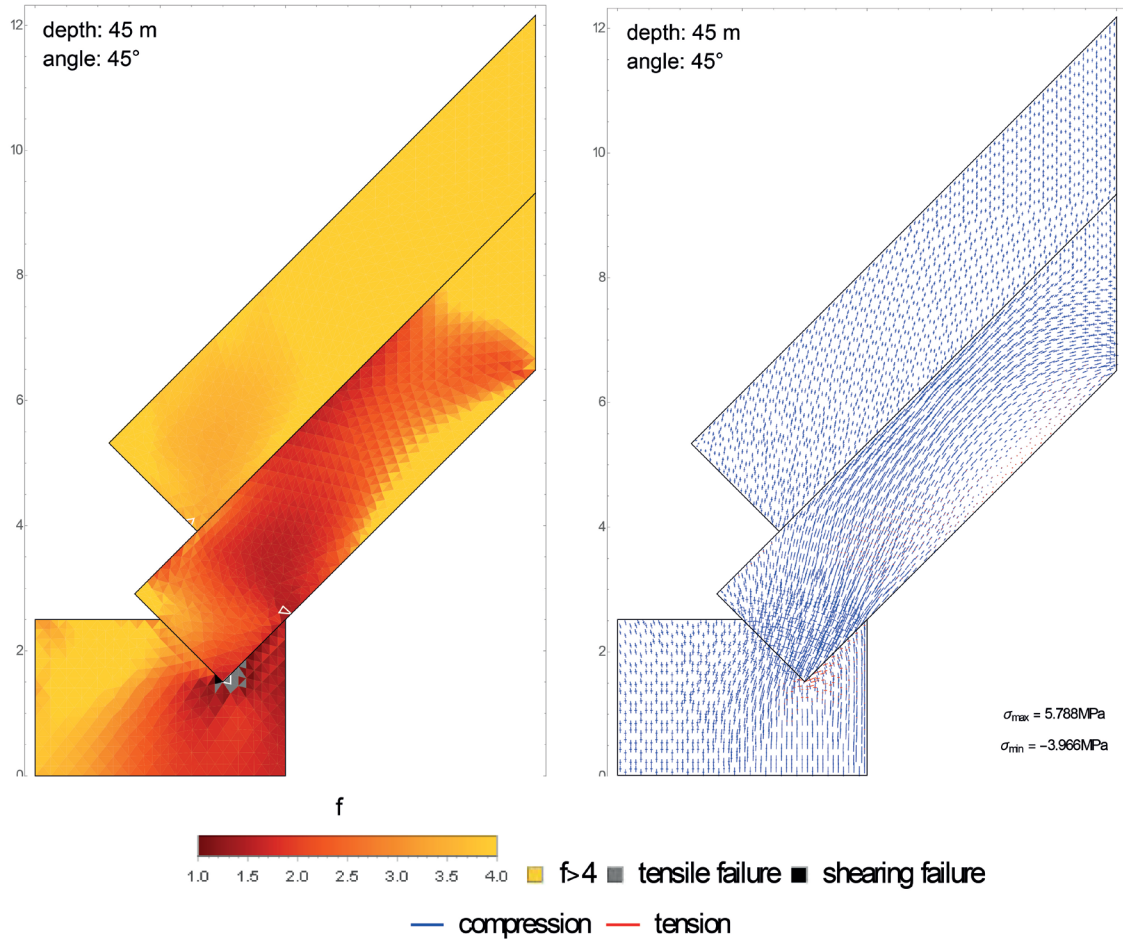


Annex 3

Safety factor and corresponding stress distribution for a vault with two layers of rafters for different angles and a depth of 45 m (zones contoured in white presents the minimum safety factor in the abutment or in the rafter).

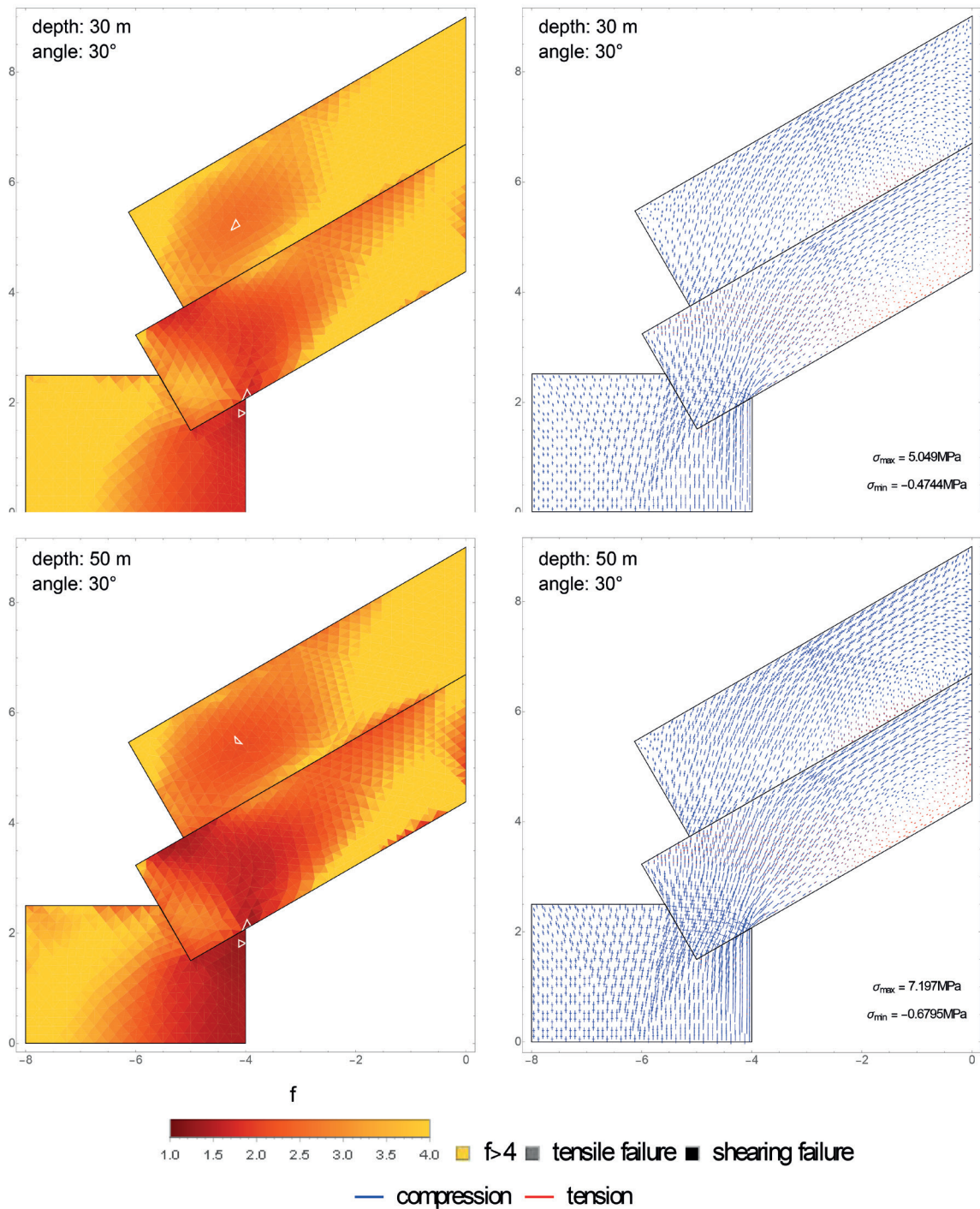


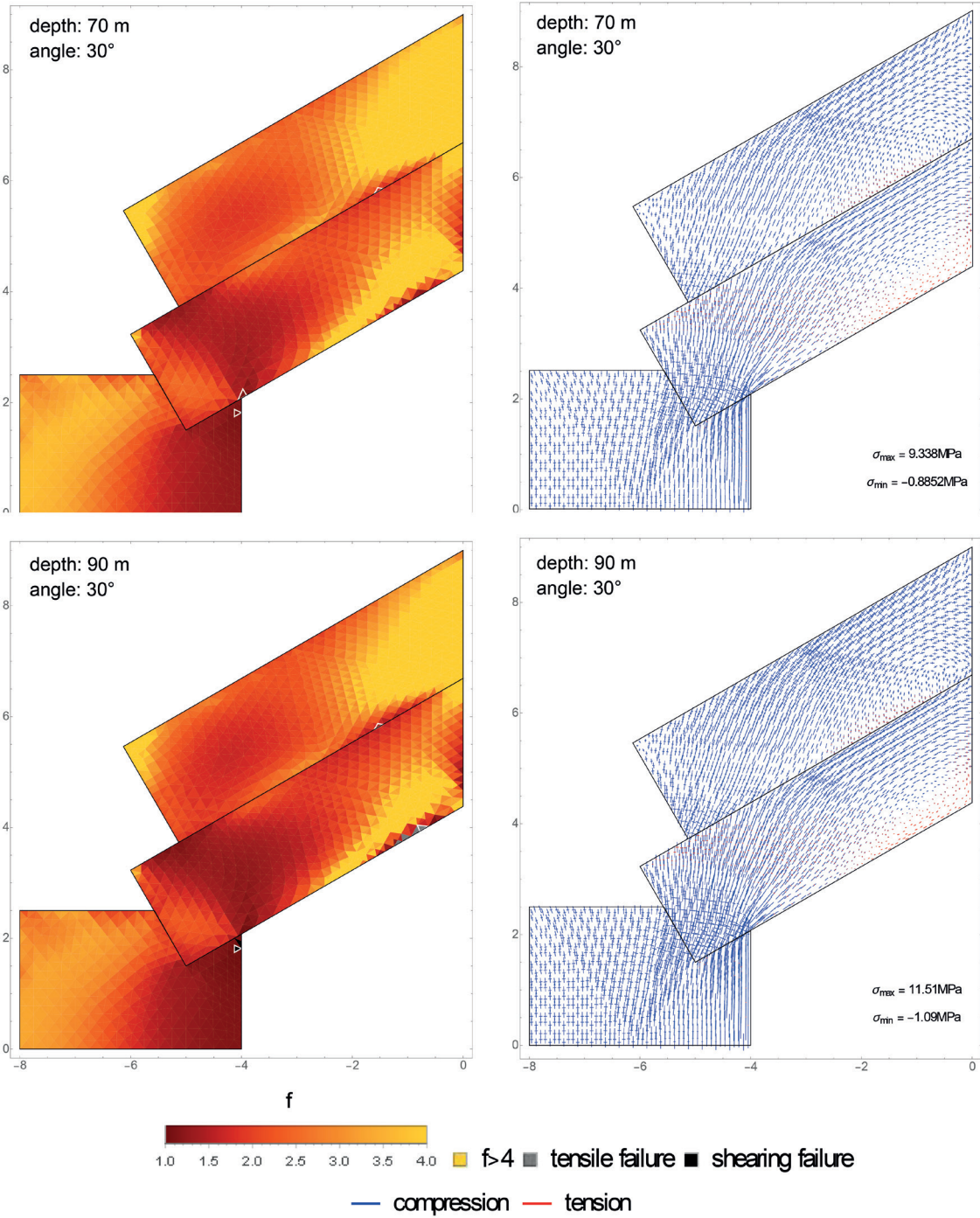




Annex 4

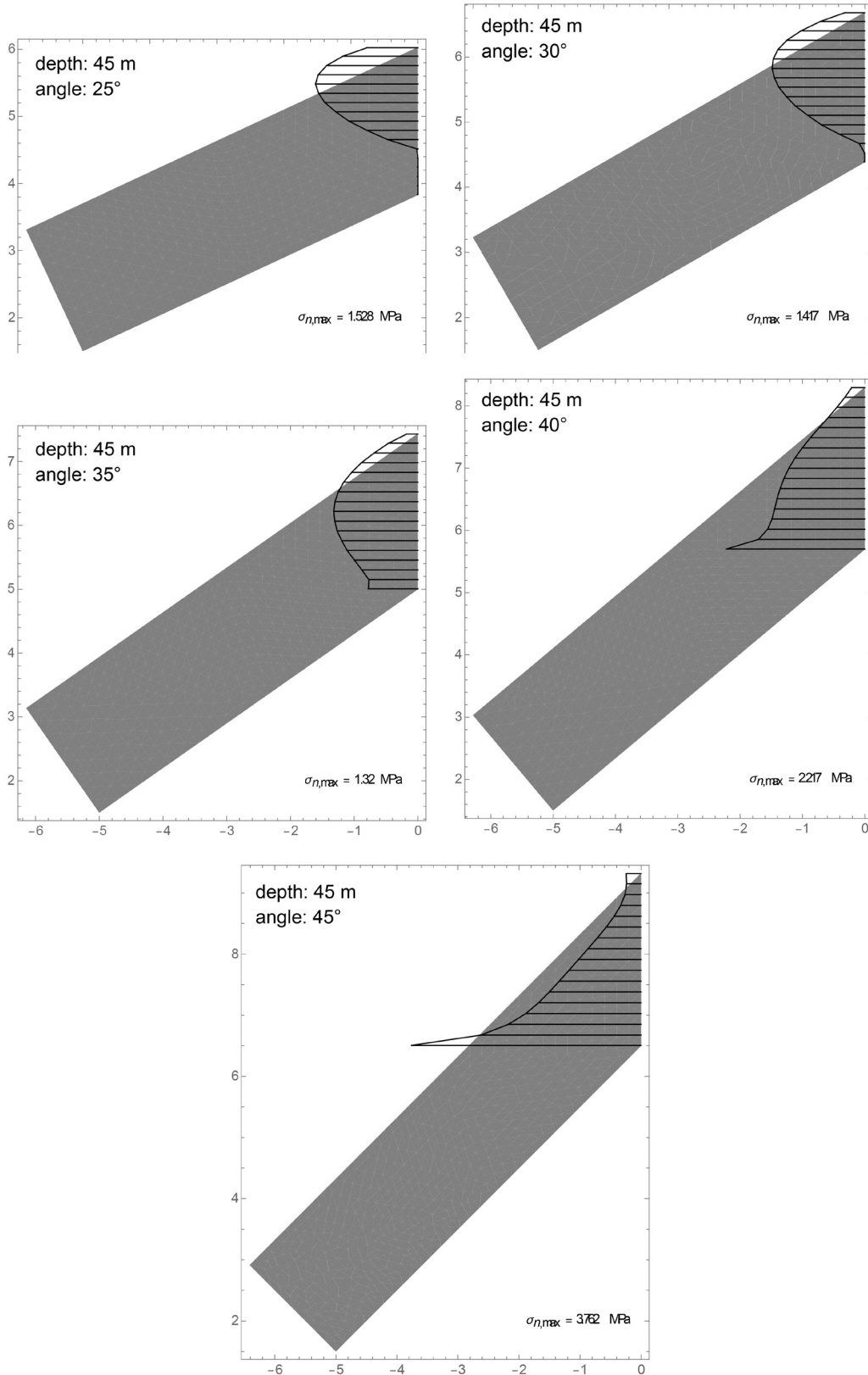
Safety factor and corresponding stress distribution for a vault with two layers of rafters for different depths and an angle of 30° (zones contoured in white presents the minimum safety factor in the abutment or in the rafter).





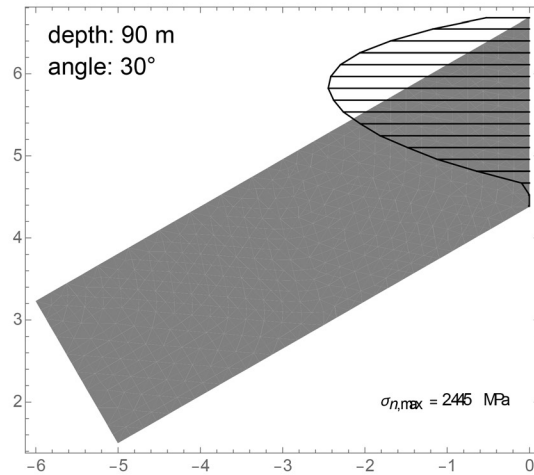
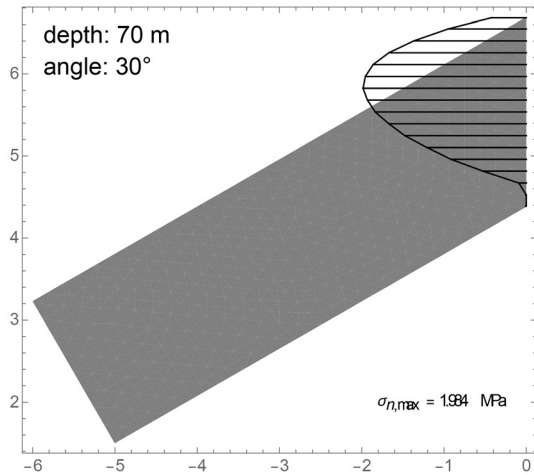
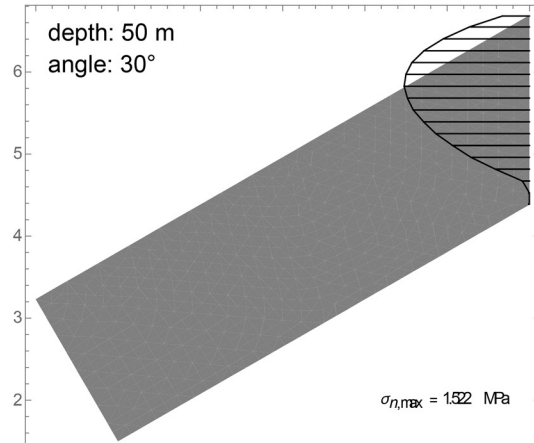
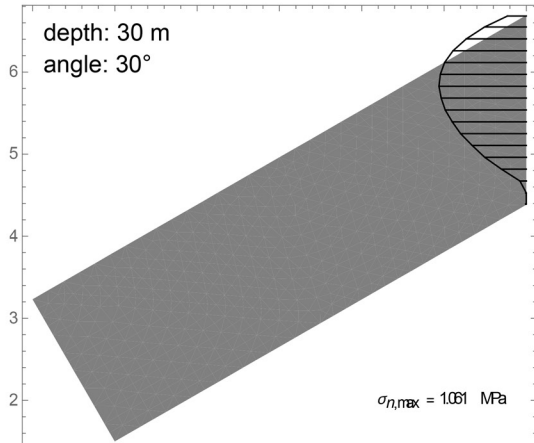
Annex 5

Normal (compressive) stress distribution on the vertical joint for a single layer of rafters for a depth of 45 m.



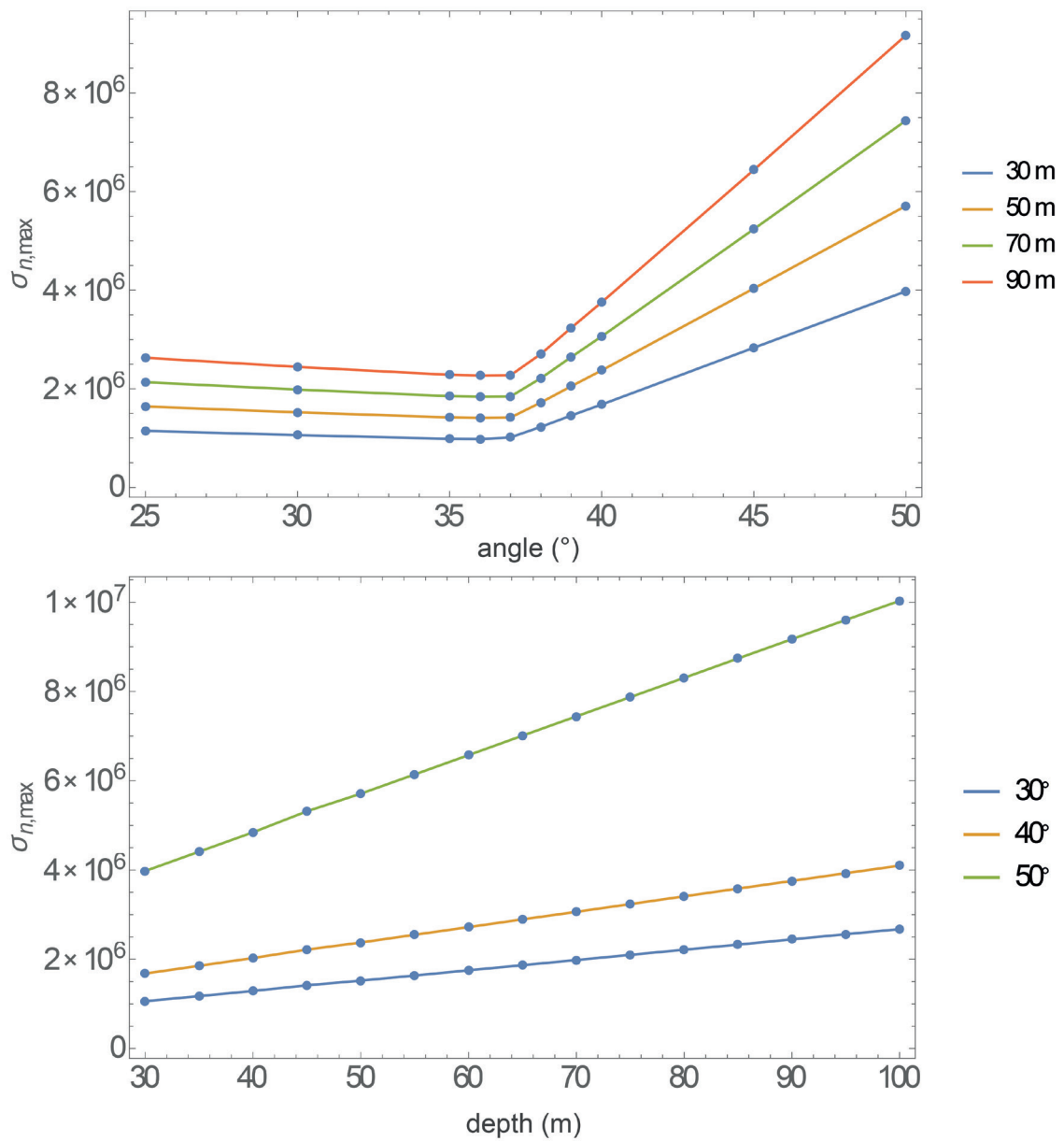
Annex 6

Normal (compressive) stress distribution on the vertical joint for a single layer of rafters for an angle of 30° .



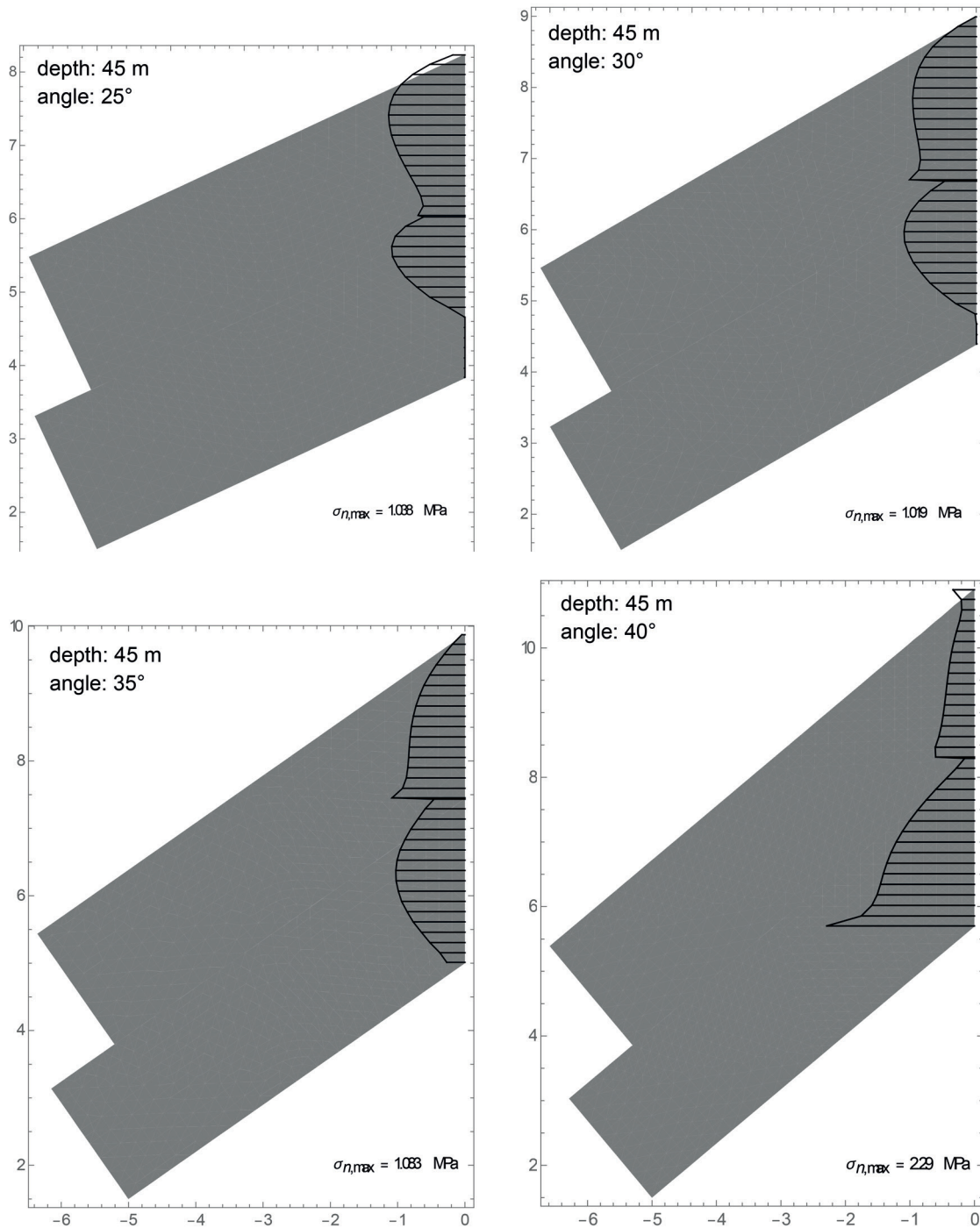
Annex 7

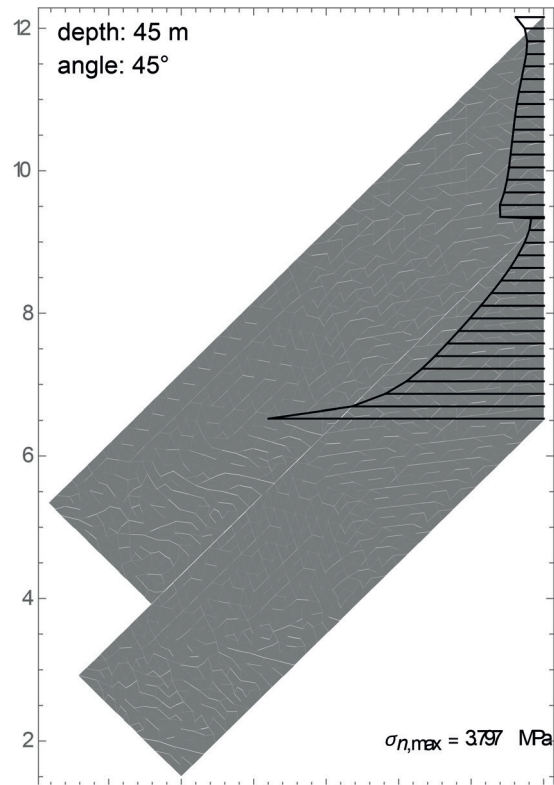
Maximum normal stress on vertical joint evolution with depth and angle (one layer).



Annex 8

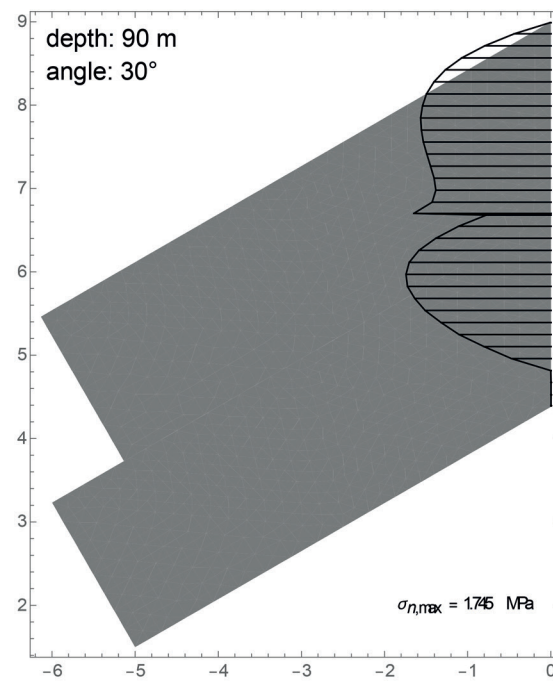
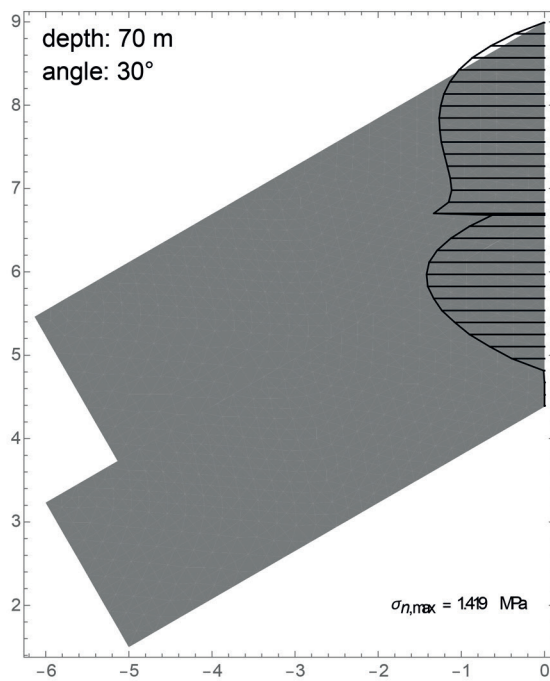
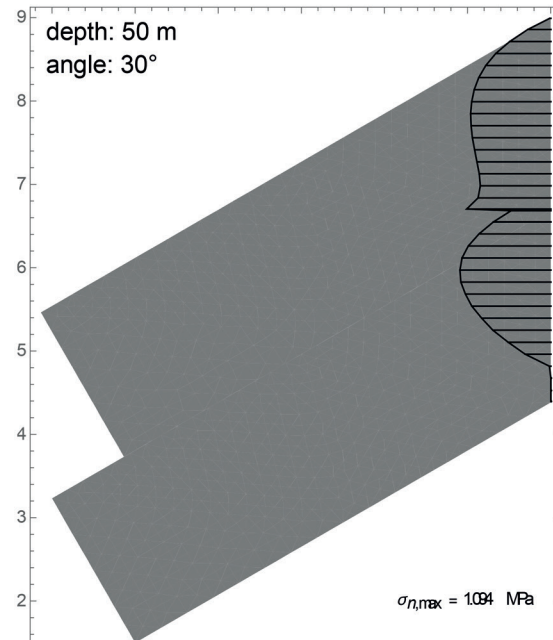
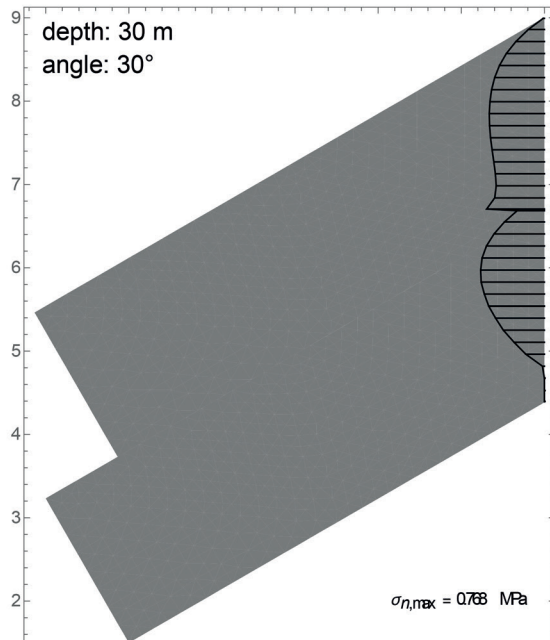
Normal (compressive) stress distribution on the vertical joint for a vault with two layers for a depth of 45 m.





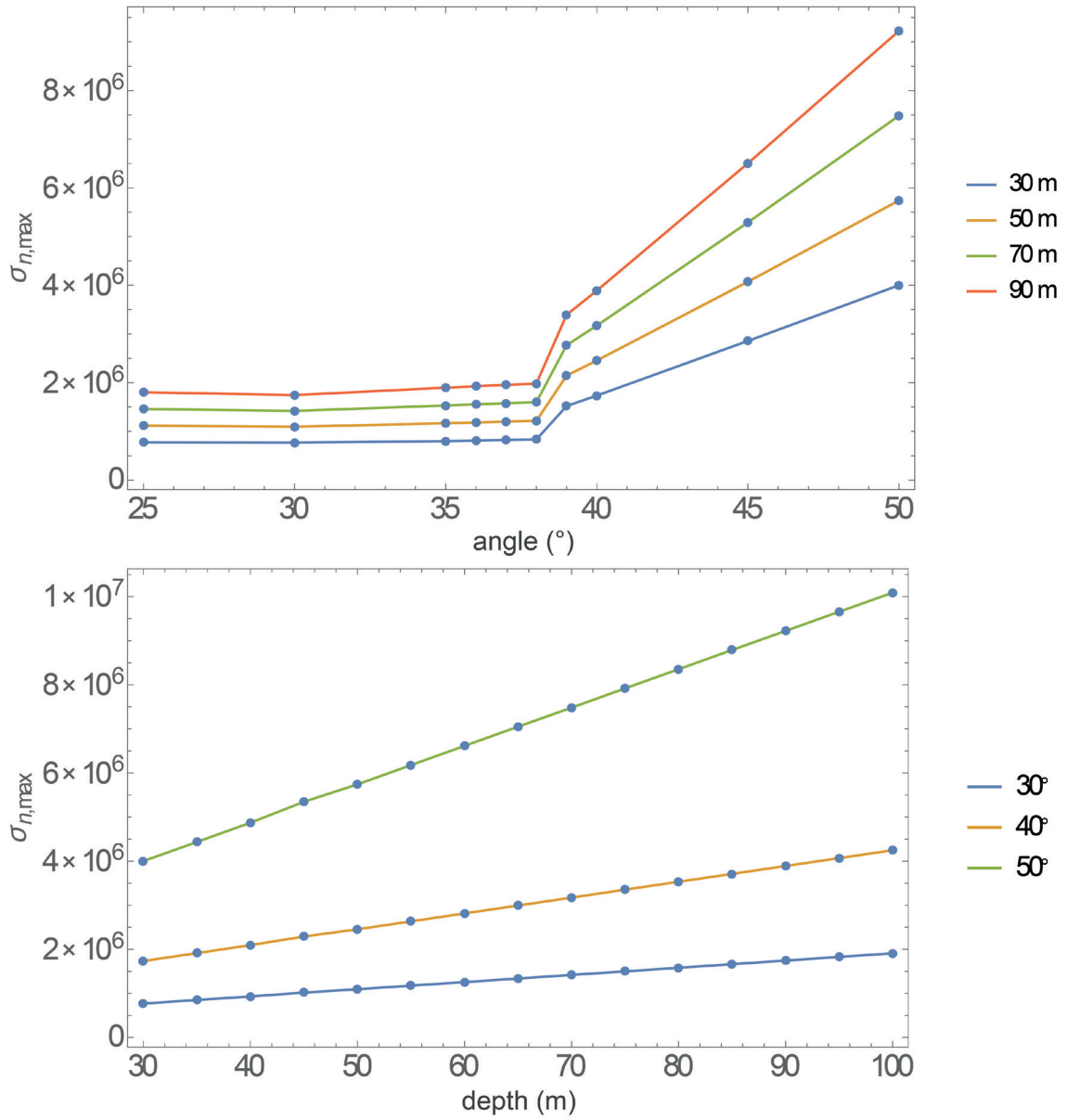
Annex 9

Normal (compressive) stress distribution on the vertical joint for a vault with two layers for an angle of 30° .



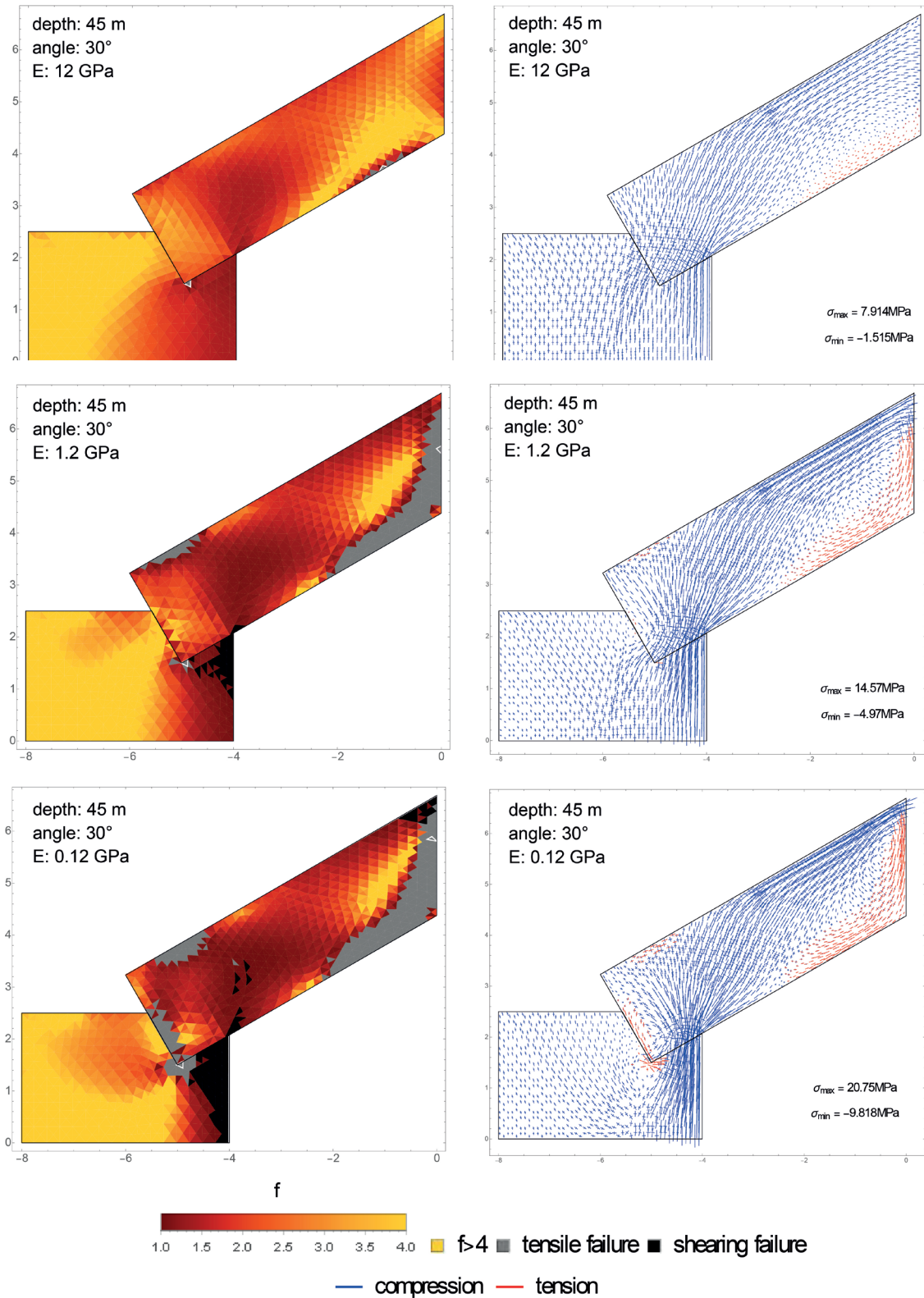
Annex 10

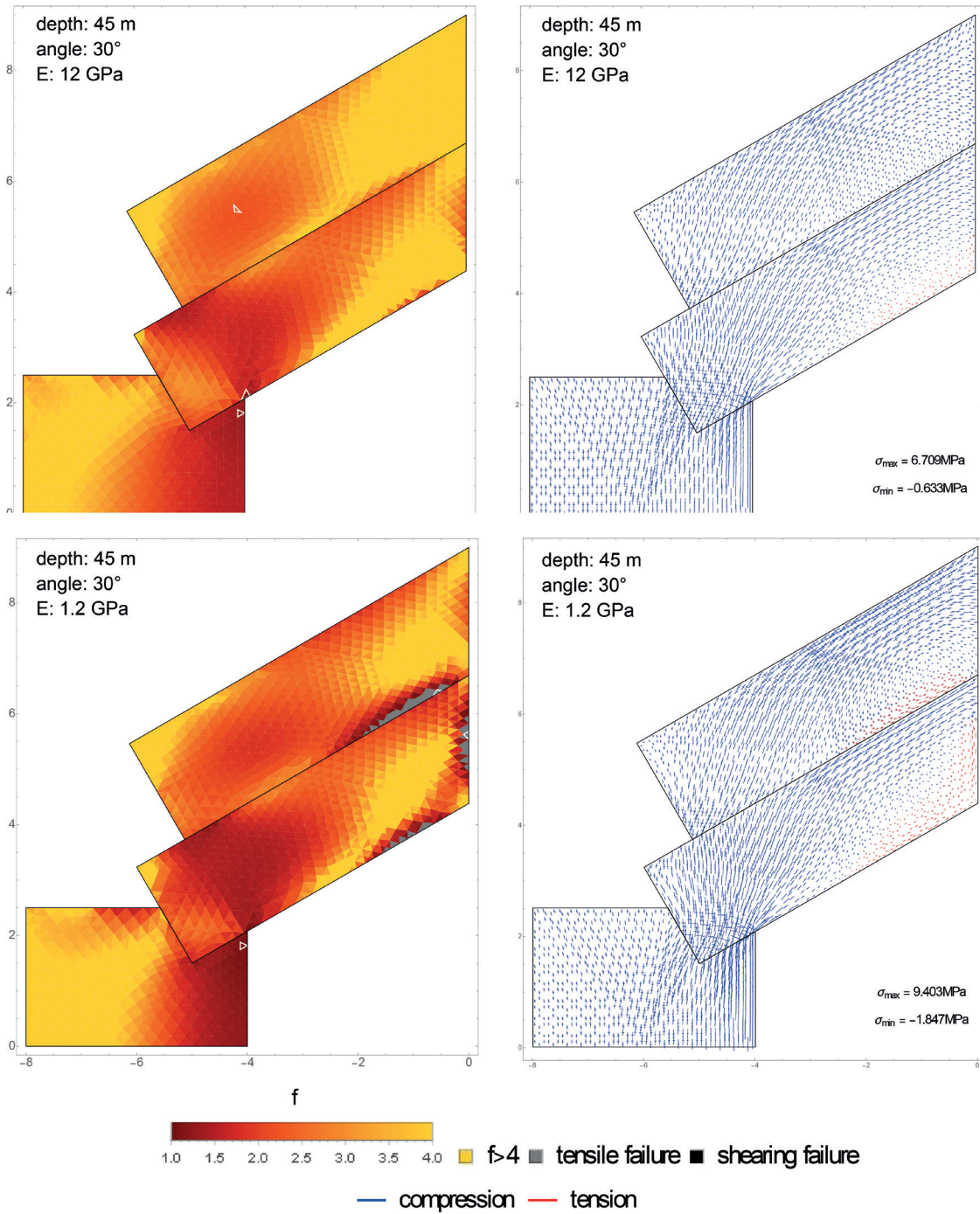
Maximum normal stress on vertical joint evolution with depth and angle (two layers).

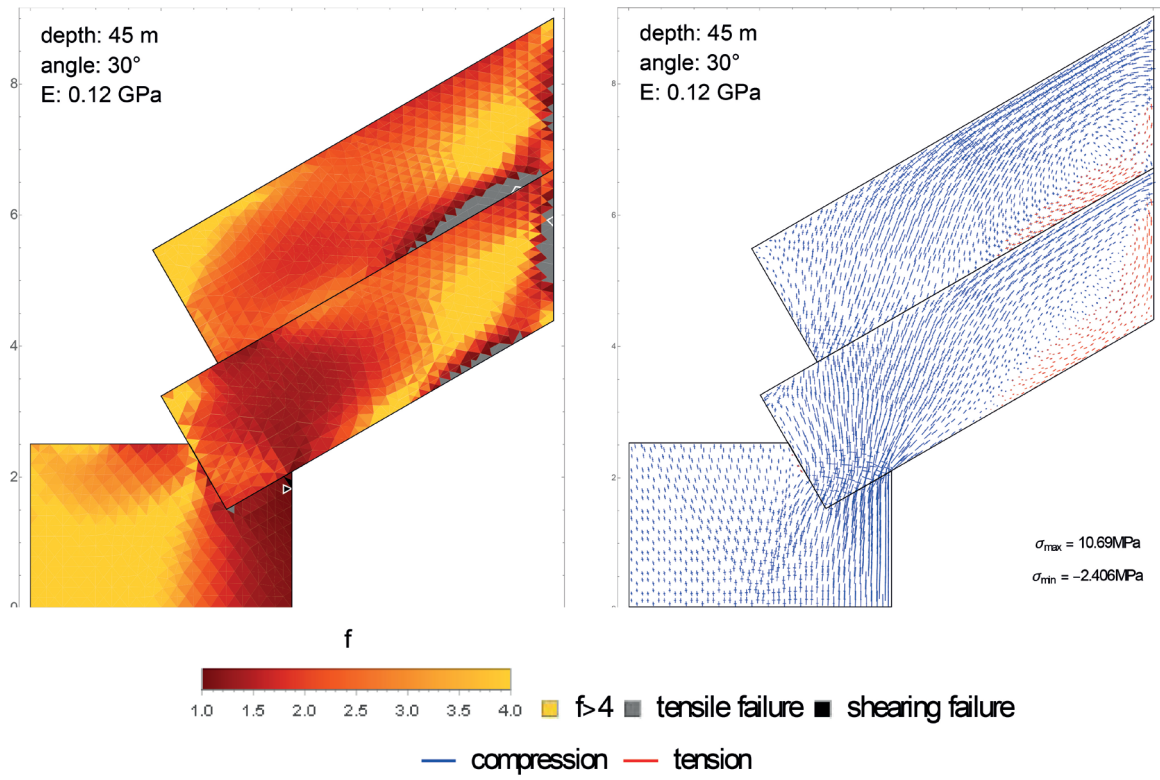


Annex 11

Safety factor and stress distribution for one layer and two layers with a decreasing Young modulus of the surroundings.

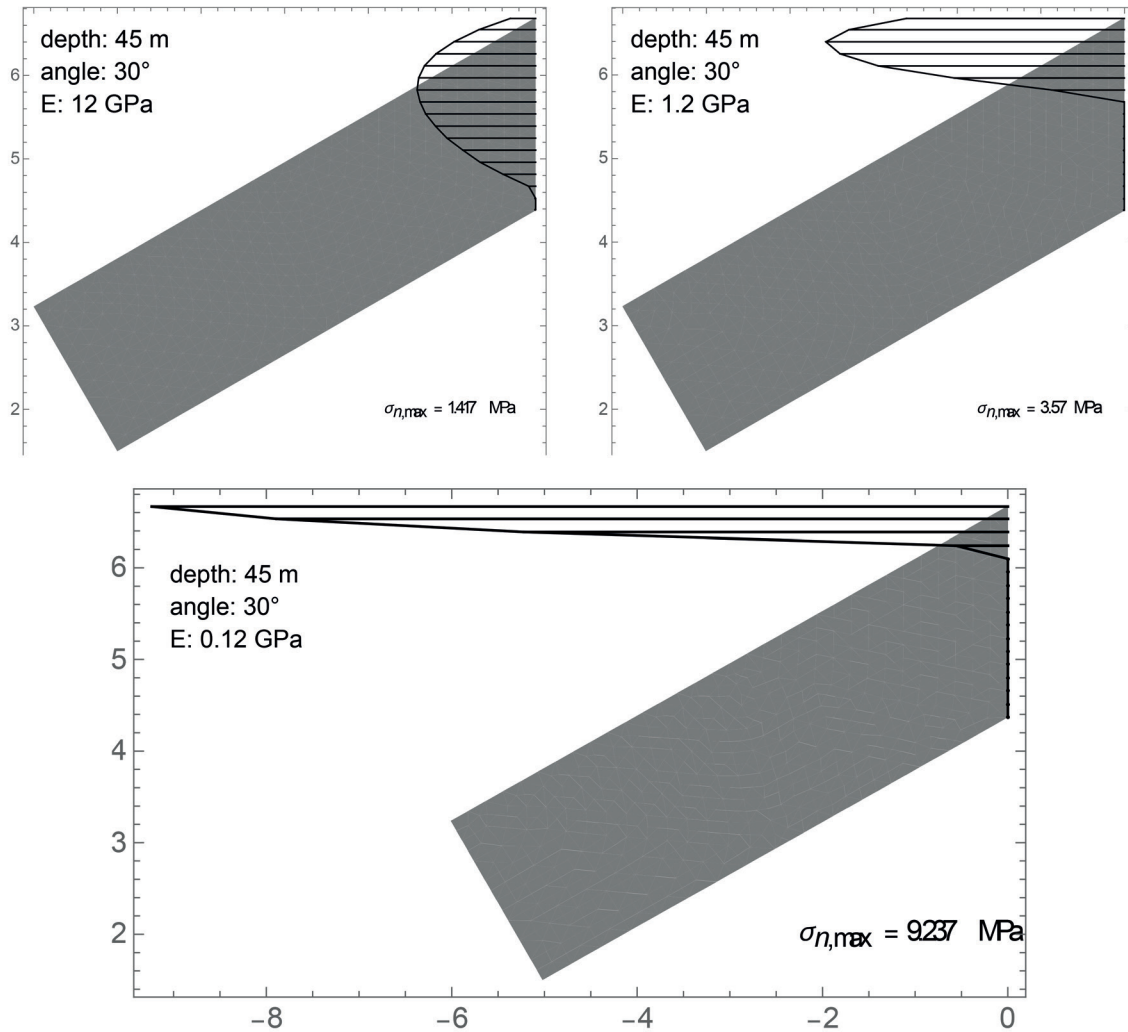






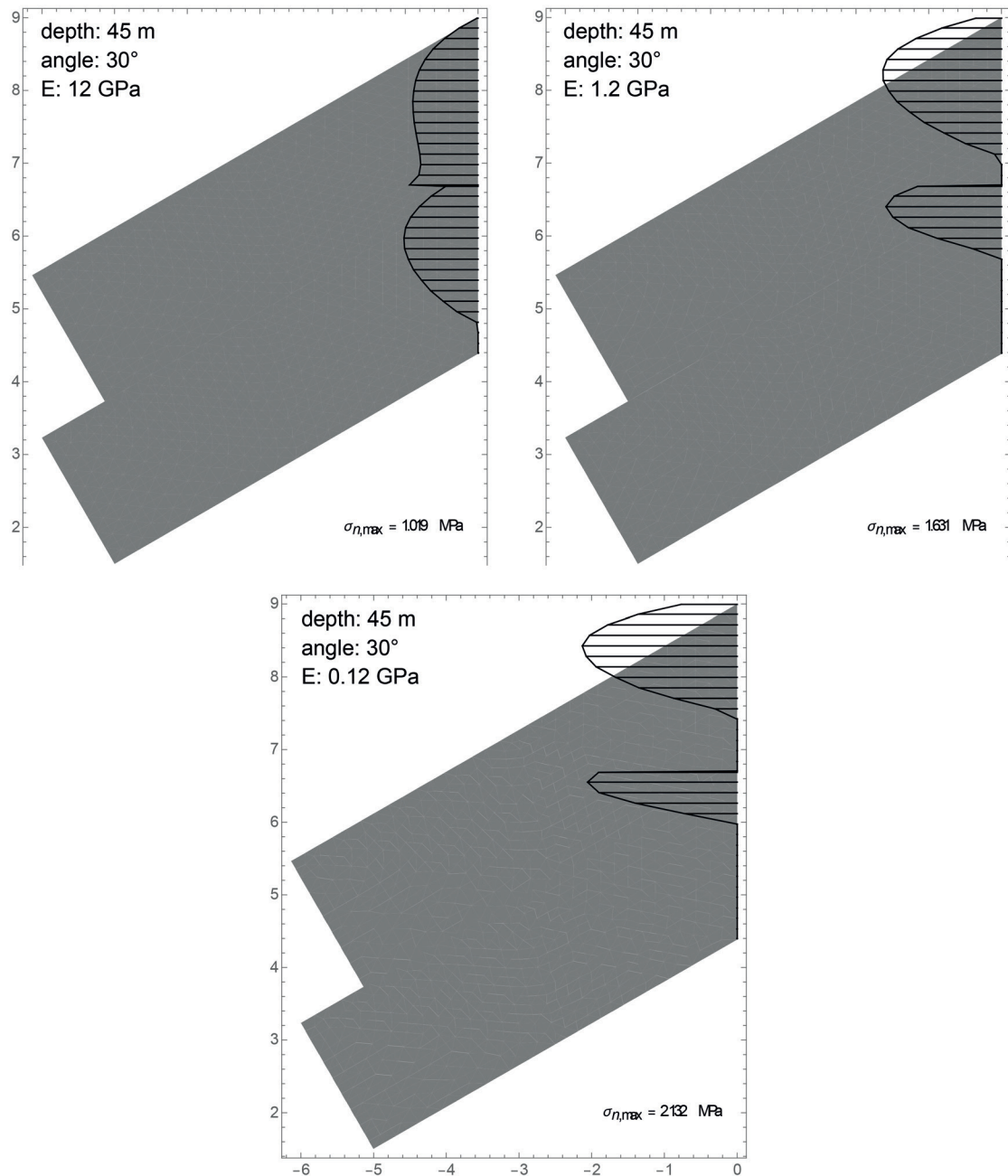
Annex 12

Normal (compressive) stress distribution on the vertical joint for one layer of rafters with the Young modulus of the surroundings decreasing



Annex 13

Normal (compressive) stress distribution on the vertical joint for a vault with two layers with the Young modulus of the surroundings decreasing.



Erratum

Vertical contact between rafters (p. 74)

The article text incorrectly reads “The real rafters mentioned above, however, have angles of inclination of approximately 40° and yet display some opening, which suggests slightly different masonry characteristics’.

The inclination of the vault rafters above the King’s Chamber is in fact 33° , so that the behavior of the King’s Chamber’s vault does in fact correspond with the results from the modelling. This issue of vault gap separation nevertheless deserves to be studied in further detail, because the vault of the Queen's Chamber is built at a similar inclination of 32° , but the ridge line interface did not separate. There are several factors that may explain this discrepancy, including different loadings, additional rafter layers above, or slightly different masonry characteristics in the surrounding matrix.